Neuron, Vol. 48, 45–62, October 6, 2005, Copyright ©2005 by Elsevier Inc. DOI 10.1016/j.neuron.2005.08.032

Phosphorylation of Neurogenin2 Specifies the Migration Properties and the Dendritic Morphology of Pyramidal Neurons in the Neocortex

Randal Hand,[1,4] Dante Bortone,[1,4] Pierre Mattar,[2] Laurent Nguyen,[3] Julian Ik-Tsen Heng,[3] Sabrice Guerrier,[1] Elizabeth Boutt,[1] Eldon Peters,[1] Anthony P. Barnes,[1] Carlos Parras,[3] Carol Schuurmans,[2] François Guillemot,[3] and Franck Polleux[1,*]

[1]Department of Phamacology
Neuroscience Center
University of North Carolina
Chapel Hill, North Carolina 27599
[2]University of Calgary
Calgary, Alberta
Canada T2N 4N1
[3]Division of Molecular Neurobiology
NIMR- MRC
Mill Hill
United Kingdom

Summary

The molecular mechanisms specifying the dendritic morphology of different neuronal subtypes are poorly understood. Here we demonstrate that the bHLH transcription factor *Neurogenin2* (*Ngn2*) is both necessary and sufficient for specifying the dendritic morphology of pyramidal neurons in vivo by specifying the polarity of its leading process during the initiation of radial migration. The ability of *Ngn2* to promote a polarized leading process outgrowth requires the phosphorylation of a single tyrosine residue at position 241, an event that is neither involved in *Ngn2* direct transactivation properties nor its proneural function. Interestingly, the migration defect observed in the *Ngn2* knockout mouse and in progenitors expressing the Ngn2^{Y241F} mutation can be rescued by inhibiting the activity of the small-GTPase RhoA in cortical progenitors. Our results demonstrate that *Ngn2* coordinates the acquisition of the radial migration properties and the unipolar dendritic morphology characterizing pyramidal neurons through molecular mechanisms distinct from those mediating its proneural activity.

Introduction

The astonishing diversity of dendritic morphologies characterizing distinct neuronal subtypes underlies their sophisticated signal processing and computational properties (Hausser et al., 2000). Although substantial progress has been made in characterizing the late, activity-dependent phase of dendritic branching and adaptation of the size of the dendritic arbor relative to presynaptic inputs (reviewed in Wong and Ghosh, 2002), the molecular mechanisms specifying the dendritic shape characterizing neuronal subclasses are still poorly understood in vertebrates (Jan and Jan, 2003; Scott and Luo, 2001; Whitford et al., 2002).

In the neocortex and hippocampus, pyramidal neurons are initially characterized by a polarized outgrowth of one major dendrite, i.e., the apical dendrite (Miller, 1981; Peters and Kara, 1985a), whereas the vast majority of cortical GABAergic interneurons undergo an unpolarized dendritic outgrowth leading to a range of multipolar, nonpyramidal dendritic morphologies (Miller, 1986; Peters and Kara, 1985b). Pyramidal and nonpyramidal neurons represent two developmentally distinct neuronal lineages generated by specialized sets of progenitors. Pyramidal neurons originate from progenitors located in the dorsal telencephalon expressing transcription factors such as *Emx1*, *Neurogenin* (*Ngn*) 1 and *Ngn2*, *Pax6*, and *Tlx1/2*. These excitatory, glutamatergic neurons migrate radially along a radial glial scaffold to reach their appropriate laminar position in an inside-first outside-last manner and have an axon projecting over long distances to subcortical or to other cortical areas. Conversely, cortical GABAergic interneurons originate from ventral telencephalic progenitors (medial and caudal ganglionic eminence [MGE and CGE, respectively]) expressing a different combination of transcription factors such as *Mash1*, *Nkx2.1*, *Lhx6*, and *Dlx1/2*. These neurons migrate tangentially into the cortex, display a variety of multipolar, nonpyramidal dendritic morphologies, and project only locally within the cortex (reviewed in Marin and Rubenstein, 2003; Schuurmans and Guillemot, 2002).

In *Drosophila*, proneural basic-Helix-Loop-Helix (bHLH) transcription factors such as *atonal* or *achaete-scute* were identified by their ability to promote neural fates in external sense organ models (Jarman et al., 1993; reviewed in Bertrand et al., 2002). Interestingly *atonal* does not have proneural activity in the fly central nervous system but instead controls the pattern of axonal branching during larval and pupal development (Hassan et al., 2000). Furthermore, although the proneural activity of bHLH transcription factors was shown to reside in the DNA binding basic region (Quan et al., 2004), there is evidence that neuronal subtype specification is controlled by residues outside the DNA binding domain in both vertebrates and invertebrates (Huang et al., 2000b; Nakada et al., 2004). In mammals, recent evidence supports the notion that the bHLH protein *Ngn2* plays a critical role not only in the acquisition of panneuronal properties (Lee and Pfaff, 2003; Nieto et al., 2001; Scardigli et al., 2001; Sun et al., 2001) but in the specification of neuronal subtypes (Fode et al., 1998, 2000; Lee and Pfaff, 2003; Ma et al., 1999; Mizuguchi et al., 2001; Parras et al., 2002; Ross et al., 2003; Scardigli et al., 2001; Schuurmans et al., 2004; Seibt et al., 2003). Specifically, a recent study demonstrated that *Ngn1* and *Ngn2* specify the expression of glutamate as the excitatory neurotransmitter in pyramidal cortical neurons (Schuurmans et al., 2004). These results raised the question of whether *Ngn2* function in cortical progenitors was limited to the specification of neurotransmitter expression or whether *Ngn2* also participates in the

*Correspondence: polleux@med.unc.edu
[4]These authors contributed equally to this work.

specification of other phenotypic traits of cortical glutamatergic neurons, such as their radial migration properties and their pyramidal dendritic morphology.

In the present study, we provide evidence that the coordinated specification of the radial migration properties and the unipolar dendritic morphology characterizing pyramidal neurons is controlled by the transcription factor *Ngn2.* Importantly, this activity is mediated in a largely DNA binding-independent manner that instead requires the phosphorylation of a tyrosine residue at position 241 in the C-terminal domain of Ngn2, a residue that is not directly involved in mediating its transactivation properties or its proneural properties. Our results demonstrate that *Ngn2* coordinates the acquisition of the radial migration properties and the unipolar dendritic morphology characterizing pyramidal neurons through molecular mechanisms distinct from those mediating its proneural activity.

Results

Neurogenin2 Is Transiently Expressed by Postmitotic Neurons during the Initiation of Radial Migration in the Subventricular Zone

It is well established that *Ngn2* mRNA is specifically expressed by cortical progenitors in both the ventricular zone (VZ) and subventricular zone (SVZ) of the dorsal telencephalon throughout neurogenesis (Fode et al., 2000; Schuurmans et al., 2004), while it is not expressed by progenitors located ventrally in the ventral telencephalon. Moreover, Ngn2 is expressed by cortical progenitors during the window of time when they commit to the neuronal lineage both in the "surface," proliferative divisions in the VZ and the "nonsurface" neurogenic divisions in the SVZ (Miyata et al., 2004; Murciano et al., 2002). Careful examination of the spatial pattern of Ngn2 expression in the cortical germinal zones at E16 (when both the VZ and SVZ are prominent) confirmed that cortical progenitors located in the VZ express Ngn2 (Figures 1A and 1J). Interestingly, Ngn2 is also expressed by a subset of cells in the SVZ and in the intermediate zone (IZ) (Figures 1A–1C). Using double immunofluorescent staining, we confirmed that a significant proportion of $Ngn2^+$ cells in the SVZ express pan-neuronal markers such as NeuN (Figures 1D–1E‴), microtubule associated protein-2, or MAP2 (Figures 1F–1G‴), and β-III tubulin, or TuJ1 (Figures 1H–1I‴). The quantification shown in Figure 1J shows that although the majority of cells expressing Ngn2 (green bars) were located in the VZ, the bulk of Ngn2-NeuN double-labeled neurons (orange bars in Figure 1J) were located primarily in the SVZ. The percentage of $Ngn2^+$ cells expressing NeuN increased almost linearly as a function of the distance from the ventricle (Figure 1K), reaching approximately 50% in the SVZ and 80% in the IZ when these neurons engage in radial migration (Noctor et al., 2004). Interestingly, Ngn2 is rapidly downregulated at the protein level once neurons reach the top of the IZ.

Neurogenin2 Is Necessary for the Specification of the Radial Migration Properties of Cortical Neurons

Recent BrdU birthdating studies demonstrated that $Ngn2^{-/-}$ embryos have a pronounced migration defect in the cortex, as shown by the ectopically deep location of cells born between E12.5 and E14.5 in the SVZ and IZ of neonatal $Ngn2^{-/-}$ cortex (Schuurmans et al., 2004). To further explore how *Ngn2* controls the radial migration properties of cortical neurons, we developed a knockin allele of *Ngn2* by replacing the entire *Ngn2* coding sequence with EGFP ($Ngn2^{KIFGP}$; see Seibt et al., 2003). Throughout neurogenesis, EGFP faithfully reports the regional expression of *Ngn2* in the dorsal telencephalon of heterozygous $Ngn2^{KIGFP/+}$ embryos with the exception that EGFP is maintained much longer in neurons and acts as a lineage tracer in the CP (Figures 2A and 2B at E14.5 and data not shown). As expected, homozygous $Ngn2^{KIGFP/KIGFP}$ embryos express approximately 2-fold more EGFP compared to $Ngn2^{KIFGP/+}$ embryos (compare Figures 2A and 2B) and represent a null with regard to Ngn2 expression (data not shown). Similar to two previously described *Ngn2* null alleles, the majority of $Ngn2^{KIGFP/KIGFP}$ mice die shortly after birth (Fode et al., 1998, 2000). We will refer to mice homozygous for this EGFP allele as $Ngn2^{-/-}$ or Ngn2 knockout in the remainder of the study.

Comparison of hematoxylin/eosin-stained sagittal sections from $Ngn2^{+/+}$ and $Ngn2^{-/-}$ neonatal cortices (Figure 2) revealed the presence of large heterotopic cell clusters in the *Ngn2* mutants that are suggestive of a neuronal migration defect (arrows in Figures 2D–2F) but not in $Ngn2^{+/+}$ controls (Figures 2C–2E). This is reinforced by the presence of streams of cells that seemed unable to exit the SVZ in the $Ngn2^{-/-}$ cortex (arrow in Figure 2F). Other heterotopias are observed at the cortico-striatal boundary (Figures 2H) and the hippocampus of the $Ngn2^{-/-}$ mice (Figure 2J) but not in control mice (Figures 2G and 2I, respectively).

To directly test whether radial migration was defective in $Ngn2^{-/-}$ embryos, we implemented a technique that combines electroporation-mediated gene transfer with in vitro organotypic slice culture (see Figure S1 in the Supplemental Data available online). This ex vivo cortical electroporation technique allows (1) the transfection of radial glial neural progenitors at reproducible efficiencies (up to 30% transfection efficiency among $nestin^+$ VZ/SVZ progenitors) and (2) specifically targets only dorsal telencephalic precursors, not GABAergic migrating interneurons (D.B., R.H., and F.P., unpublished data). By 4 DIV a single cohort of radially migrating neurons have reached their final position forming a single layer at the top of the CP (Figure S1). This recapitulates the timing displayed by layer V migrating neurons in vivo as demonstrated by birthdating studies (Berry and Rogers, 1965; Polleux et al., 1997) as well as by using the in utero electroporation technique (R.H., D.B., and F.P, unpublished data; see also Bai et al., 2003; Hasegawa et al., 2004; Hatanaka and Murakami, 2002; Kawauchi et al., 2003; Shu et al., 2004; Tabata and Nakajima, 2001).

The cortical electroporation of E14.5 $Ngn2^{-/-}$ embryos revealed a pronounced migration defect resulting in the accumulation of transfected cells in the SVZ and IZ and a failure to reach the CP (star in Figure 2L) compared to $Ngn2^{+/+}$ littermates (Figure 2K). To quantify these effects we developed an automated cell profile counting tool to compute the percentage of cell profiles

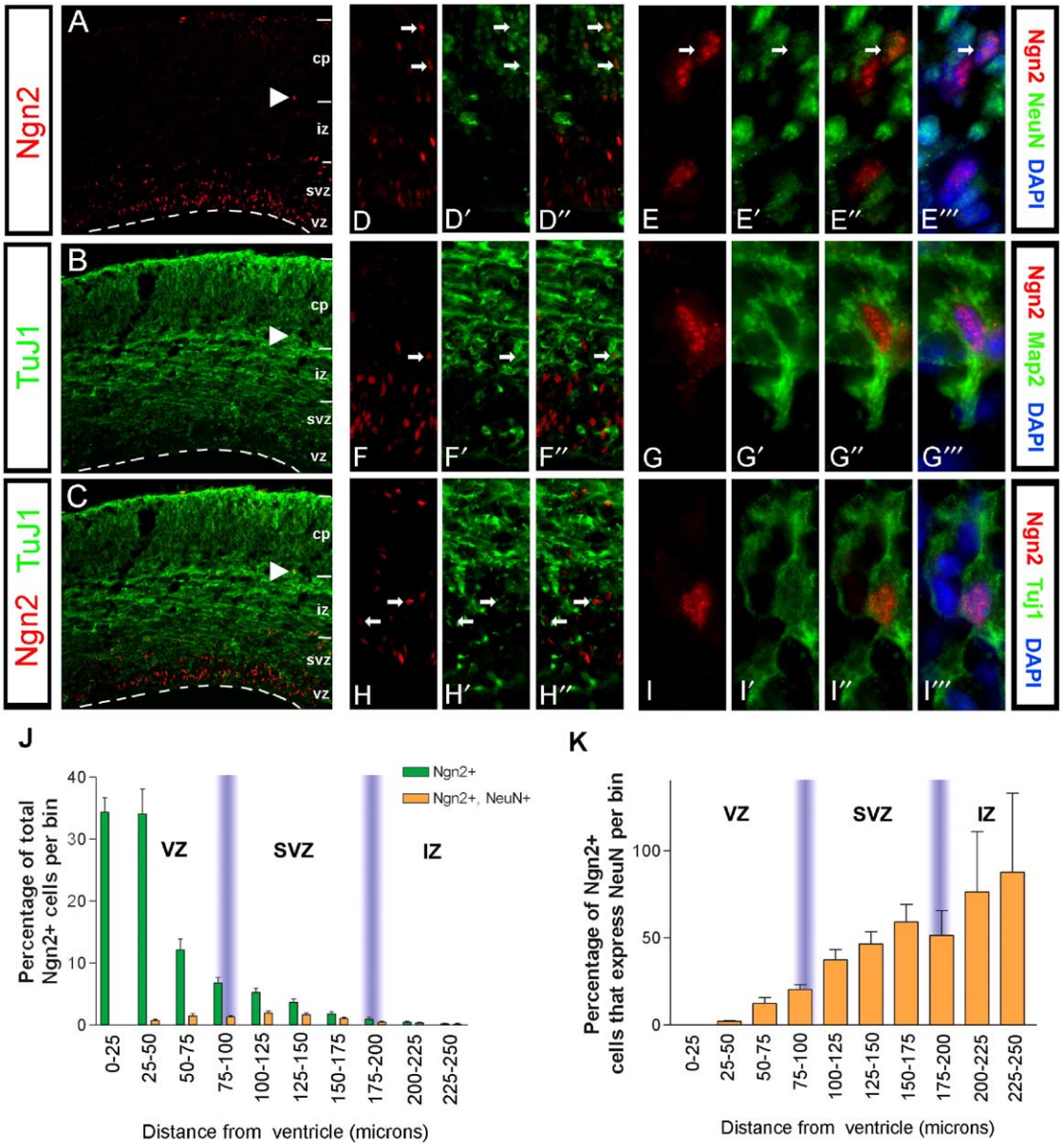

Figure 1. Neurogenin2 Is Expressed Both in Neuronal Progenitors and Early Postmitotic Neurons in the Developing Cortex

(A–C) Double immunofluorescent staining performed at embryonic day (E) 16 on cryostat sections from mouse cortex against Ngn2 protein (A) and the early neuronal marker βIII-tubulin (TuJ1) (B and C).

(D–D″ and E–E‴) Coexpression of Ngn2 (D) and NeuN (D′) in the SVZ (D–D″). Note the nuclear localization of Ngn2 in double immunopositive cells in the SVZ (arrows in [E]–[E‴]).

(F–F″ and G–G‴) Coexpression of Ngn2 (F and G) and MAP2 (F′ and G′) in the SVZ (arrow in [F″] and [G″]–[G‴]).

(H–H″ and I–I‴) Coexpression of Ngn2 (H and I) and Tuj1 (H′ and I′) confirms the presence of Ngn2$^+$ neurons in the SVZ (arrow in [F″] and [G″]–[G‴]).

(J) Quantification of the distribution of Ngn2$^+$ cells (green bars) and Ngn2/NeuN double-positive neurons (orange bars) expressed as a percentage of the total number of Ngn2$^+$ cells found in 25 μm wide bins.

(K) Quantification of the radial distribution of Ngn2-NeuN double-positive neurons calculated as a percentage of the total number of cells expressing Ngn2$^+$ in each bin.

CP, cortical plate; VZ, ventricular zone; SVZ, subventricular zone; IZ, intermediate zone.

distributed along the radial axis of the cortical wall (Figures 2M and 2N; see the Supplemental Experimental Procedures). This quantification demonstrates that after 4 DIV approximately 30% of electroporated cells successfully migrated to the CP-MZ layers in *Ngn2*$^{+/+}$ slices (Figure 2M), whereas less than 10% of electroporated cells do so in the *Ngn2*$^{-/-}$ slices (Figure 2N). In contrast a significantly higher percentage of electroporated cells remain in the lower IZ and SVZ regions of the *Ngn2*$^{-/-}$ slices (Figure 2N) compared to control *Ngn2*$^{+/+}$ slices (Figure 2M).

A limitation of this analysis is that *Ngn2* specifies the

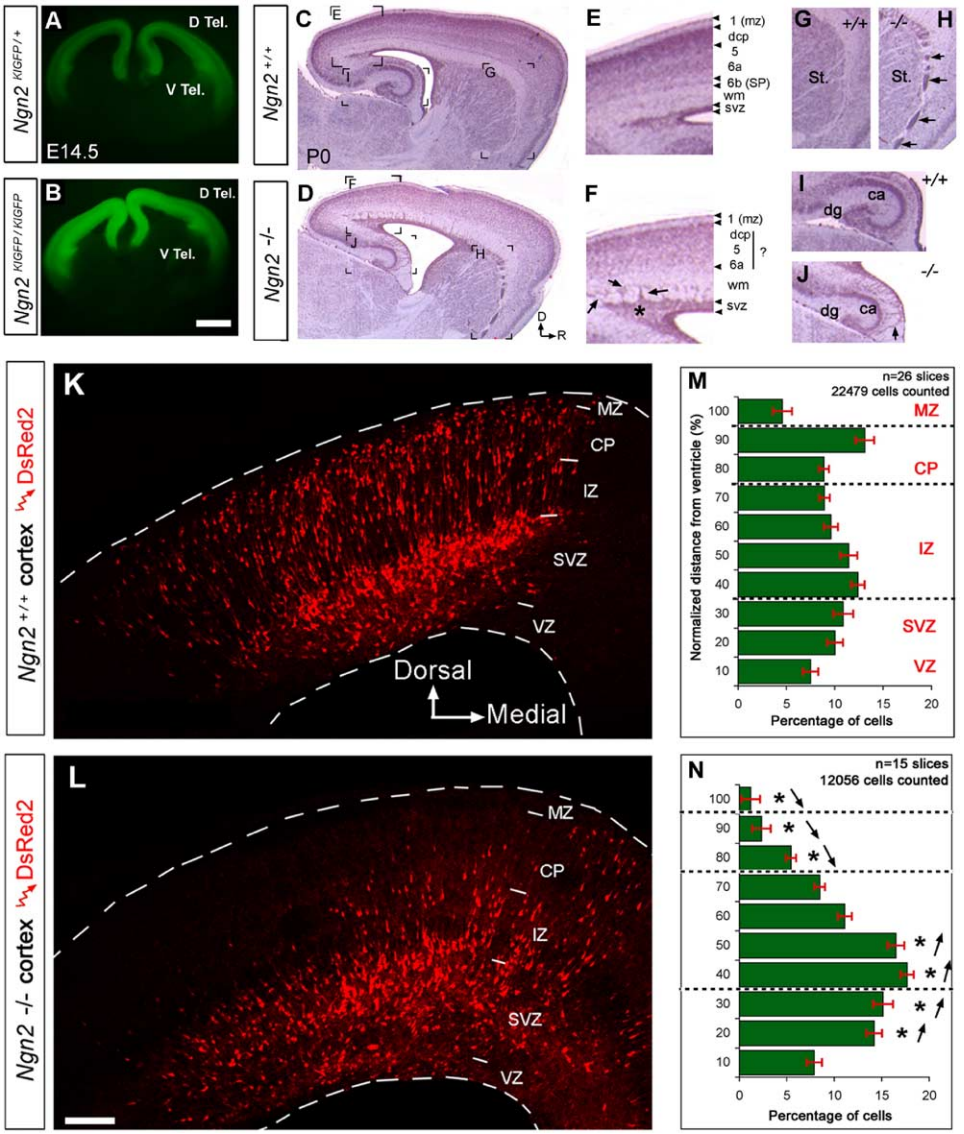

Figure 2. *Neurogenin2* Is Required In Vivo for the Proper Migration of Cortical Neurons

(A and B) EGFP epifluorescence in live coronal organotypic slices isolated from E14.5 *Ngn2*$^{KIGFP/+}$ mouse embryos (A) and *Ngn2*$^{KIGFP/KIGFP}$ mouse embryos (B) shows expression of *Ngn2* in the dorsal telencephalon (D Tel.).

(C–J) Sagittal cryostat sections from postnatal day 0 (P0) *Ngn2*$^{+/+}$ (C, E, G, and I) and *Ngn2*$^{-/-}$ (D, F, H, and J) mice counterstained with hematoxylin-eosin. At higher magnification, streams of ectopic cells (arrows in [F]) emerging from the SVZ (star in [F]) are detected in *Ngn2*$^{-/-}$ mice but not in control *Ngn2*$^{+/+}$ mice (E). Heterotopic cell clusters are also found at the cortico-striatal boundary and underneath the developing CA regions of the hippocampus of the *Ngn2*$^{-/-}$ (arrows in [H] and [J], respectively) but not the *Ngn2*$^{+/+}$ mice (G and I).

(K and L) Ex vivo electroporation of pCIG2:DsRed2 in cortical progenitors of *Ngn2*$^{+/+}$ (K) and *Ngn2*$^{-/-}$ (L) E14.5 embryos followed by organotypic culture for 4 days in vitro (DIV).

(M and N) Quantification of the distribution of DsRed2-expressing cells along the radial axis of E14.5 *Ngn2*$^{+/+}$ (M) and *Ngn2*$^{-/-}$ slices (N) after 4 DIV. *$p < 0.001$ χ^2 test comparing corresponding bins.

ca, Ammon's horn regions of the hippocampus; dg, dentate gyrus; MZ, marginal zone; St., striatum; wm, white matter. Scale bars, 100 μm (K and L).

molecular identity of dorsal telencephalic neurons (reviewed in Schuurmans and Guillemot, 2002). Dorsal progenitors in E12.5 *Ngn2* knockouts upregulate *Mash1*, a bHLH transcription factor normally expressed by ventral telencephalic progenitors of the GE specifying the GABAergic neurons fate (Fode et al., 2000; Parras et al., 2002; Schuurmans et al., 2004). Therefore, these long-term molecular fate changes in *Ngn2*$^{-/-}$ cortical progenitors could indirectly affect the migratory properties of their daughter neurons.

Acute Conditional Deletion of *Neurogenin2* in Cortical Progenitors Alters the Initiation of Radial Migration

In order to circumvent these long-term effects, we performed an acute deletion of *Ngn2* expression in corti-

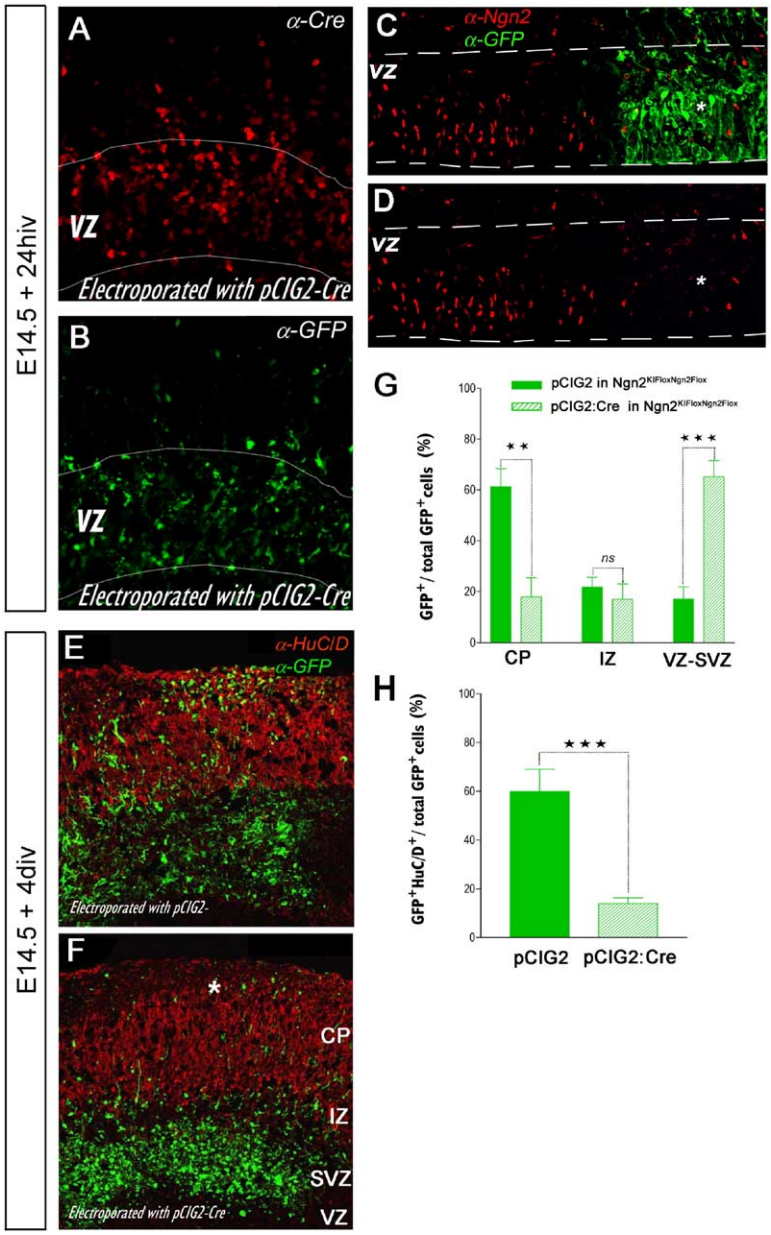

Figure 3. Acute Deletion of Ngn2 Expression in E14.5 Cortical Progenitors Impairs Radial Migration

(A and B) Ex vivo electroporation of E14.5 dorsal telencephalic progenitors using a pCIG2: Cre-recombinase-IRES-EGFP followed by in vitro organotypic slice culture for 24 hr in vitro results in high-level of coexpression of Cre-recombinase (A) and EGFP (B).

(C and D) Electroporation of Cre-recombinase in cortical progenitors from *Ngn2*^{KIFloxNgn2Flox} E14.5 embryos (C) results in a pronounced downregulation of Ngn2 protein expression (star in [C] and [D]) in the VZ.

(E and F) Acute deletion of Ngn2 expression in cortical progenitors results in a pronounced decrease in the number of neurons reaching the CP (star in [F]) compared to control electroporation (EGFP only) in *Ngn2*^{KIFloxNgn2Flox} E14.5 progenitors (E). Red: immunofluorescence against the neuronal marker HuC/D in (E) and (F).

(G) Quantification of the percentage of EGFP^{+} cells located in the VZ-SVZ, IZ, or CP compartments. For both (G) and (H), n = 7 slices, unpaired t test, **p < 0.01, ***p < 0.001.

(H) Quantification of the percentage of GFP^{+} cells expressing the neuronal marker HuC/D reveals a pronounced proneural defect in progenitors where Ngn2 was deleted (pCIG2::Cre) compared to control transfected progenitors (pCIG2).

cal progenitors by using Cre-mediated deletion of *Ngn2* specifically in dorsal telencephalic progenitors. This was achieved by using ex vivo electroporation of a plasmid expressing nuclear targeted-Cre recombinase-IRES-EGFP in E14.5 cortical progenitors harboring a new conditional allele of Ngn2 (homozygous *Ngn2*^{KIFloxNgn2Flox} mice). As shown in Figures 3A and 3B, our electroporation technique leads to high levels of Cre-recombinase and EGFP coexpression in E14.5 cortical progenitors in less than 24 HIV. As shown in Figures 3C and 3D, Ngn2 protein expression is markedly decreased in *Ngn2*^{KIFloxNgn2Flox} cells expressing Cre. Interestingly, E14.5 *Ngn2*^{KIFloxNgn2Flox} cortical slices electroporated with Cre and cultured for 4 DIV present a pronounced neuronal migration defect with very few neurons reaching the CP (Figures 3F and 3G) compared to control (EGFP only) electroporation (Figures 3E and 3G). These results reinforce our conclusion that *Ngn2* specifies the migration properties of cortical neurons.

One caveat of this interpretation is that the acute loss of Ngn2 function affects the percentage of electroporated EGFP-expressing cells expressing pan-neuronal markers such as HuC/D as an index of its proneural activity (Figure 3H). This result suggests a strong proneural defect upon acute inactivation of Ngn2 expression in cortical progenitors, which is compatible with the well-documented function of *Neurogenins* (reviewed in Bertrand et al., 2002). The dominant proneural function of this class of *Neurogenins* represents the main limitation in defining their other functions in neuronal subtype specification. To overcome this, we performed a structure-function analysis of Ngn2 in order to uncouple the proneural activity of Ngn2 from its potential function in the phenotypic specification of neuronal subtypes.

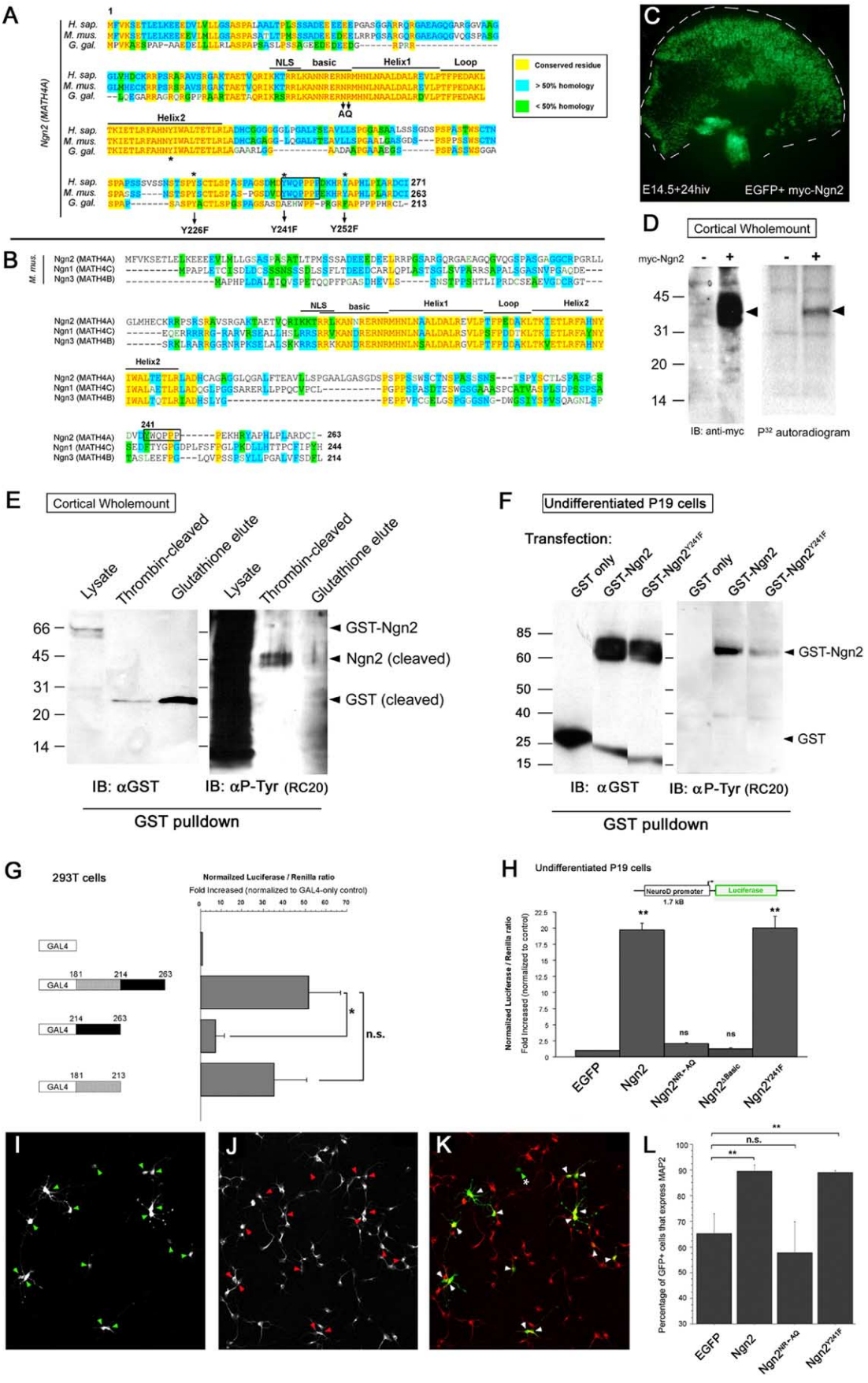
A
Ngn2 (MATH4A)
H. sap.
M. mus.
G. gal.
Conserved residue
> 50% homology
< 50% homology
NLS
basic
Helix1
Loop
Helix2
AQ
Y226F
Y241F
Y252F
B
M. mus.
Ngn2 (MATH4A)
Ngn1 (MATH4C)
Ngn3 (MATH4B)
241
C
E14.5+24hiv
EGFP+ myc-Ngn2
D
Cortical Wholemount
myc-Ngn2
IB: anti-myc
P32 autoradiogram
E
Cortical Wholemount
Lysate
Thrombin-cleaved
Glutathione elute
GST-Ngn2
Ngn2 (cleaved)
GST (cleaved)
IB: αGST
IB: αP-Tyr (RC20)
GST pulldown
F
Undifferentiated P19 cells
Transfection:
GST only
GST-Ngn2
GST-Ngn2Y241F
GST
G
293T cells
Normalized Luciferase / Renilla ratio
Fold Increased (normalized to GAL4-only control)
n.s.
H
Undifferentiated P19 cells
NeuroD promoter
Luciferase
1.7 kB
Normalized Luciferase / Renilla ratio
Fold Increased (normalized to control)
EGFP
Ngn2
Ngn2NR+AQ
Ngn2ΔBasic
Ngn2Y241F
I
J
K
L
Percentage of GFP+ cells that express MAP2

Neurogenin2 Is Tyrosine Phosphorylated In Vivo

The alignment of chick (*Gallus gallus*), mouse (*Mus musculus*), and human (*Homo sapiens*) Ngn2 protein sequences revealed a complete conservation of the bHLH domains and a partial conservation of undefined amino- (N-) and carboxy- (C-) terminal domains (Figure 4A). Interestingly, the N- and C-terminal domains of mouse Ngn2 are highly divergent from Ngn1 and Ngn3, two closely related homologs (Figure 4B). In order to isolate potential residues outside the DNA binding domain that might mediate neuronal subtype specification, we first determined whether Ngn2 was posttranslationally modified and specifically if it was phosphorylated in cortical progenitors. Using electroporation of *myc*-tagged Ngn2 in E14.5 cortical progenitors followed by 24 hr of cortical wholemount culture in vitro in the presence of γ^{32}P-labeled ATP and *myc* immunoprecipitation (Figure 4C), we found that Ngn2 is phosphorylated in cortical precursors (Figure 4D).

To examine the putative phosphorylation sites in Ngn2, we used a sequence- and structure-based prediction program (Blom et al., 1999; see Supplemental Experimental Procedures), which predicted 15 potential serine residues, 4 threonine residues, and 3 tyrosine residues displaying a significant ($p > 0.90$) probability of phosphorylation. Using electroporation of a GST-Ngn2 fusion protein in cortical precursors followed by GST-pulldown and thrombin cleavage of Ngn2 from GST, we found that Ngn2 is tyrosine phosphorylated in cortical precursors (Figure 4E). Using GST-pulldown in undifferentiated P19 cells to increase the protein yield, we found that tyrosine 241 is likely to be the major site for tyrosine phosphorylation in Ngn2 because mutation of this residue into a phenylalanine residue (Ngn2^{Y241F}) drastically reduces the signal detected by anti-phosphotyrosine immunoblotting (Figure 4F) compared to control full-length Ngn2.

Therefore, in the rest of this study we focused our effort on the effects of mutating tyrosine 241. In addition, mutations of the two other tyrosine residues presenting a high probability to get phosphorylated (Y226F and Y252F) did not produce any detectable effects on the acquisition of neuronal migration properties or dendritic morphologies (see Figure S5 and data not shown). Interestingly, tyrosine 241 (1) is part of a proline-rich motif (YWQPPPP, boxed in Figure 4A) that constitutes a predicted binding site for SH2-containing proteins, (2) is mammalian specific (not conserved in chick but perfectly conserved in human), and (3) is specific to Ngn2 (not present in mouse Ngn1 or mouse Ngn3; see box in Figure 4B).

In order to test the requirement of the DNA binding properties of Ngn2 in mediating some of its biological functions, we produced double substitution in basic residues 123–124 (e.g., Ngn2$^{NR->AQ}$). This mutation was previously shown to abolish DNA binding of Neurogenins to direct target promoter sequences (Lee and Pfaff, 2003; Sun et al., 2001) without interfering with its nuclear localization (see Figure S2).

First we tested whether tyrosine 241 was located within the transactivation domain (TAD) of Ngn2. To our knowledge, the TAD of Ngn2 has never been mapped. We performed a standard TAD mapping using a modified Gal4-UAS system (Figure 4G). The TAD of most proneural bHLH transcription factors lies in the proximal or the distal portion of the C-terminal domain of

Figure 4. Neurogenin2 Is Tyrosine Phosphorylated in Cortical Precursors

(A) Alignment of human (*Homo sapiens* NP_076924), mouse (*Mus musculus* NP_033848), and chick (*Gallus gallus* NP_990127) Ngn2 protein sequences. The asterisks indicate the position of the four tyrosine residues conserved in mouse and human Ngn2 proteins. The arrowheads indicate the tyrosine residues presenting a high probability of phosphorylation that we mutated into phenylalanine residues.

(B) Alignment of mouse Ngn2 (MATH4A; NP_033848), Ngn1 (MATH4C; NP_035026), and Ngn3 (MATH4B; NP_033849) protein sequences reveals a high level of conservation of their bHLH domains but a low level of conservation of the N- and C-terminal domains including the YWQPPPP motif in the C-terminal domain of Ngn2 (boxed in [A] and [B]), which is not found in Ngn1 or Ngn3.

(C) Photomicrograph showing the high electroporation efficiency of *myc*-tagged Ngn2 (*myc*-Ngn2-IRES-EGFP) obtained by ex vivo electroporation of E14.5 dorsal telencephalic progenitors subsequently cultured as wholemount for 24 hr in vitro (HIV).

(D) Anti-*myc* immunoprecipitation (IP) of Ngn2 in E14.5 cortical progenitors as shown above. Minus lane: control (EGFP only) electroporation. Right panel: ^{32}P autoradiogram of telencephalic wholemount cultures performed in the presence of γ^{32}P-labeled ATP reveals the presence of a phosphorylated protein corresponding to *myc*-Ngn2 (arrowhead at 36–40 kDa; n = 3).

(E) A GST-Ngn2 fusion protein was expressed using cortical electroporation at E14.5 followed by 24 hr of wholemount in vitro culture as shown in (C). GST-pulldown using glutathione-beads (line 1) leads to the detection of a product corresponding to GST-Ngn2 (65 kDa) using anti-GST immunoblotting. Cleavage of the GST-Ngn2 fusion protein bound to the beads by thrombin releases a small amount of GST (lane 2 at 25 kDa) and a product corresponding to Ngn2, which is detected by using an anti-phosphotyrosine antibody (Recombinant PY20 i.e., RC20 lane 5). Note that GST is efficiently released by glutathione elution (lane 3) and is not tyrosine phosphorylated (lane 6).

(F) Transfection of undifferentiated P19 cells with GST-, GST-Ngn2 fusion, or GST-Ngn2^{Y241F} fusion followed by GST-pulldown using glutathione-beads, elution, and immunoblotting with anti-GST antibody (left blot) or anti-phosphotyrosine antibody (RC20) demonstrates that tyrosine 241 is the major tyrosine phosphorylation site in Ngn2.

(G) Mapping of the transcriptional activation domain of mouse Ngn2 in HEK 293T cells using the Gal4-UAS-Luciferase system. Gal4-Ngn2$^{[181-213]}$ fusion protein (but not Gal4-Ngn2$^{[214-263]}$) is able to transactivate a UAS-Luciferase reporter to a similar extent as Gal4-Ngn2$^{[181-263]}$, suggesting that the minimal transactivation domain is located between residues 181 and 213. *$p < 0.01$ Mann-Whitney nonparametric test (n = 6); n.s., nonsignificant.

(H) Full-length Ngn2 as well as Ngn2^{Y241F} induces a robust 20-fold increase (compared to control, **$p < 0.001$ Mann-Whitney test) in transactivation of the 1.7 kB *NeuroD* promoter (Huang et al., 2000a). Both Ngn2$^{NR->AQ}$ and Ngn2$^{\Delta basic}$ (complete deletion basic domain) fail to transactivate this promoter in undifferentiated P19 cells.

(I–K) Immunofluorescence staining for EGFP (I) and MAP2 (J) was used to assess the proportion of E14.5 cortical progenitors differentiating into postmitotic neurons in different experimental conditions after culturing dissociated E14.5 progenitors for 5 DIV.

(L) Histogram of the percentage of neurons (MAP2$^+$) derived from EGFP$^+$ precursors expressing the indicated constructs. A minimum of 200 cells from four independent experiments were counted for each construct; **$p < 0.01$; n.s., nonsignificant; χ^2 analysis.

the protein (Sharma et al., 1999). Therefore, we designed three Gal4 fusion proteins containing, respectively, (1) the entire C-terminal tail of Ngn2 (residues 181–263), (2) the proximal part of the C-terminal tail (residues 181–213; gray in Figure 4G), and (3) the distal domain of the C-terminal tail (residues 214–263; black in Figure 4G). Using a normalized UAS-Luciferase/Renilla reporter assay, we found that the first half of the C-terminal tail proximal to the second helix (181–213) displays transactivation properties comparable to the entire C-terminal tail (Figure 4G). Interestingly, the distal portion encompassing residues 214–263 (including tyrosine 241) did not have any significant transactivation properties (Figure 4G).

To directly assess the transactivation properties of the mutant forms of Ngn2 used in this study, we used the 1.7 kb promoter region of *NeuroD* previously shown to be strongly transactivated by Ngn3 (Huang et al., 2000a). We found that Ngn2 strongly transactivates the *NeuroD* promoter in undifferentiated P19 cells (Figure 4H; on average 20-fold, $p < 0.01$ Mann Whitney test, $n = 3$), whereas $Ngn2^{NR->AQ}$ and $Ngn2^{\Delta basic}$ (presenting a complete deletion of the basic domain) both failed to transactivate this promoter (Figure 4H). Interestingly, the mutation of tyrosine 241 did not interfere with Ngn2-mediated transactivation of the *NeuroD* promoter (Figure 4H).

Tyrosine 241 of Neurogenin2 Is Not Involved in Mediating Its Proneural Activity

Next we wanted to assess the functional effect of mutating tyrosine 241 on the proneural function of *Ngn2*. To do this, E14.5 cortical progenitors were electroporated, dissociated, and cultured for 5 days in vitro at medium cell density (Figures 4I–4K). Our quantitative analysis revealed that under our serum-free culture conditions, overexpression of Ngn2 significantly increases the bias of progenitors to differentiate into $MAP2^+$ neurons (approximately 90%; $n = 481$ cells from three independent experiments; Figure 4L) compared to control EGFP-only transfected progenitors (63%; $n = 357$ from three independent experiments; Figure 4L). Importantly, expression of $Ngn2^{NR->AQ}$ was unable to promote neuronal differentiation ($n = 509$ cells; four independent experiments; Figure 4L), whereas expression of $Ngn2^{Y241F}$ had a proneural activity that was undistinguishable from full-length Ngn2 ($n = 377$ cells; four independent experiments; Figure 4L). These results demonstrate that the proneural activity of Ngn2 is (1) at least partially dependent on its DNA binding properties as previously shown (Lee and Pfaff, 2003; Sun et al., 2001) and (2) independent of tyrosine 241 phosphorylation.

Ngn2 Specifies the Radial Migration Properties of Cortical Progenitors in a DNA Binding Independent Manner

We used the ex vivo cortical electroporation technique to study the radial migration properties of neurons generated by cortical progenitors expressing mutant forms of Ngn2. Overexpression of wild-type Ngn2 in E14.5 cortical progenitors significantly increases the proportion of cells recruited to the SVZ and the proportion of neurons initiating radial migration and accumulating in the CP (Figures 5B and 5F) compared to control (Figures 5A and 5E). Surprisingly, expression of $Ngn2^{NR->AQ}$ did not impair the radial migration properties of E14.5 cortical neurons compared to full-length Ngn2 (Figures 5C and 5G). Importantly, expression of $Ngn2^{Y241F}$ in E14.5 cortical progenitors nearly abolished the radial migration of cortical neurons. These cells accumulated in the IZ and seemed unable to penetrate into the CP (Figures 5D and 5H). Therefore, expression of $Ngn2^{Y241F}$, but not $Ngn2^{NR->AQ}$, phenocopies the complete and the conditional loss of *Ngn2* function (see Figures 2 and 3). It is unlikely that the radial migration arrest of $Ngn2^{Y241F}$ expressing neurons is due to an indirect effect on the radial scaffold because both the number and morphology of radial glial processes are unaffected by expression of $Ngn2^{Y241F}$ after short- (36 HIV) and long-term (4 DIV) slice cultures (Figure S3).

These results show that the inhibition of radial migration resulting from the expression $Ngn2^{Y241F}$ in cortical progenitors is dominant over endogenously expressed Ngn2. To confirm this, we performed a set of coelectroporations expressing different ratios of full-length Ngn2 and $Ngn2^{Y241F}$ in vivo. When expressed at a 1:1 or even a 10:1 ratio over full-length Ngn2, $Ngn2^{Y241F}$ (Figures S4B and S4C, respectively) significantly inhibits radial migration compared to control electroporation of wild-type Ngn2 alone (Figure 4A). We conclude that $Ngn2^{Y241F}$ acts as a dominant negative.

Expression of $Ngn2^{Y241F}$ Impairs the Polarity and Nucleokinesis of Radially Migrating Neurons

To gain further insight into the cellular mechanisms underlying the function of the tyrosine 241 in Ngn2, we coupled the ex vivo cortical electroporation technique with time-lapse confocal microscopy. We used this technique to document the dynamics of radial migration of neurons expressing EGFP (and endogenous wild-type Ngn2; Figure 6A and Movie S1) or $Ngn2^{Y241F}$ (Figure 6B and Movie S2). This analysis reveals that progenitors expressing $Ngn2^{Y241F}$ are able to transit from the SVZ into the IZ, but instead of engaging radial migration, some cells (red arrowhead in Figure 6B) display a striking defect in the polarity of their leading process outgrowth (yellow arrow in Figure 6B) as well as a failure to undergo nucleokinesis (three cells pointed to in Figure 6B and Movie S1). Our quantification demonstrates that cells expressing $Ngn2^{Y241F}$ display a significant decrease in the rate of cell body translocation (Figure S5A) and a significant increase in the rate of leading process branching (Figure S5B) compared to progenitors expressing endogenous, wild-type Ngn2.

Rescue of the Migration Defect Due to *Ngn2* Loss of Function by Inhibition of RhoA Function

A recent substractive hybridization screen led to the identification of several Ngn2-target genes in the developing cortex (Mattar et al., 2004). Interestingly, several of these putative Ngn2-target genes are critical for radial migration, such as *Doublecortin* (*Dcx*; Bai et al., 2003; des Portes et al., 1998; Gleeson et al., 1998). However, several other candidate genes have no known function in regulating neuronal migration, such as two

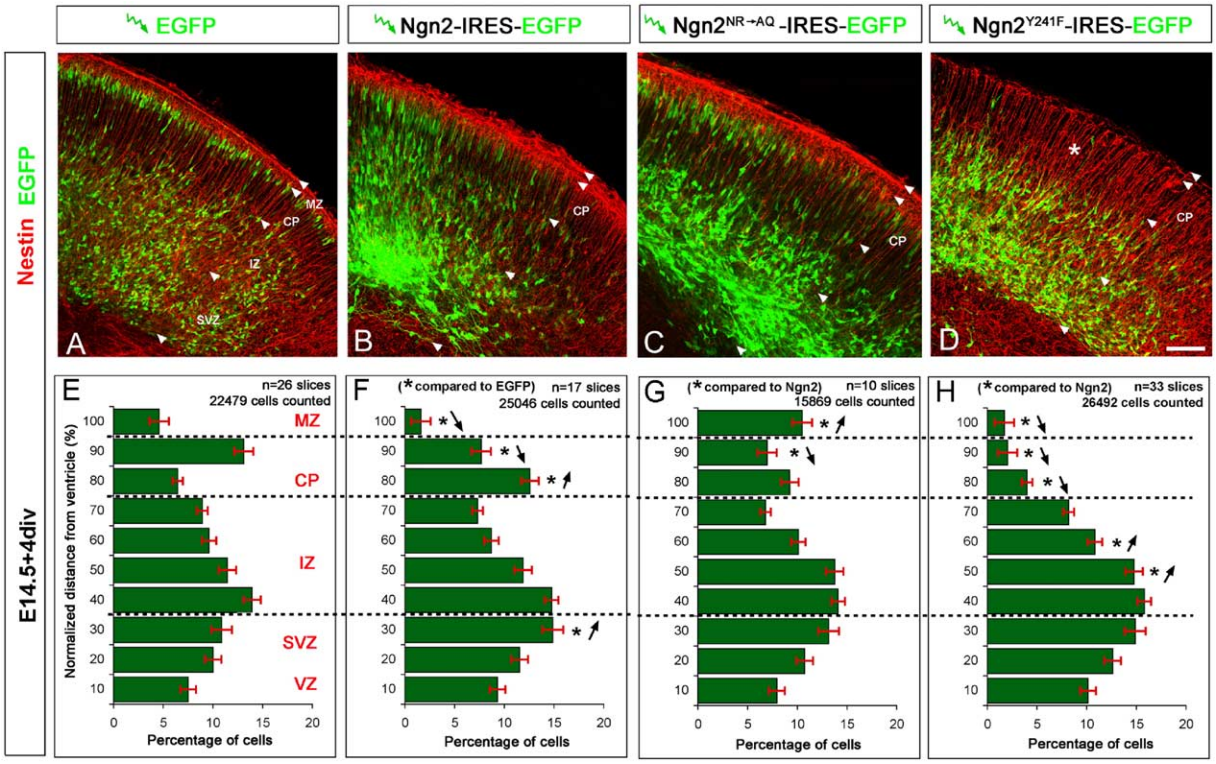

Figure 5. Phosphorylation of Tyrosine 241 in Ngn2 Is Necessary to Specify the Radial Migration Properties of Cortical Progenitors

(A) Ex vivo electroporation of E14.5 cortical progenitors followed by organotypic slice culture for 4 DIV (see also Figure S1) allows the visualization of the radial migration properties of a single cohort of neurons to the top of the CP. Red counterstaining is anti-Nestin immunofluorescence revealing the intact structure of the radial glial scaffold in all four conditions.

(B and C) Electroporation of full-length Ngn2 or Ngn2$^{NR->AQ}$ increases the number of cortical progenitors engaging in radial migration in the IZ and reaching the CP.

(D) Electroporation of Ngn2^{Y241F} results in a premature arrest of migration in the IZ (star) beneath the CP.

(E–H) Histograms of the distribution of EGFP^{+} cells along the radial extent of the cortical wall (normalized as a percentage). Error bars represent standard error to the mean. *$p < 0.01$; χ^2 comparing equivalent bins.

Scale bar value in (A)–(D), 200 μm.

Rho family GTPase activating proteins (Rho-GAPs) called *RhoGAP5* (also called *ARHGAP5* or *p190 RhoGAPb*) and *formin binding protein 2* (*FNBP2*; Katoh, 2004; also called *srGAP2* Coyle et al., 2004; Wong et al., 2001). Interestingly, *FNBP2* is specifically downregulated in cortical progenitors of E13.5 Ngn2 knockout mice compared to wild-type littermates (Mattar et al., 2004). Rho-GAPs act as negative regulators of small-GTPase activity (Ridley et al., 2003). Interestingly, the small-GTPase RhoA is specifically expressed at high levels by cortical progenitors but is sharply downregulated during the initiation of radial migration in the IZ (Olenik et al., 1999). Given the known function of activated-RhoA in inhibiting non-neuronal cell migration (Arthur and Burridge, 2001) and the downregulation of two Rho-GAPs in Ngn2 knockout cortical progenitors, we hypothesized that (1) inhibition of RhoA activity is required to initiate radial migration and therefore that (2) a failure to upregulate the expression of RhoGAPs such as *RhoGAP5* or *FNBP2*/*srGAP2* could lead to a reduced inhibition of RhoA activity in *Ngn2*$^{-/-}$ cortical progenitors, impairing their ability to initiate radial migration upon cell cycle exit.

In order to test this hypothesis, we used the electroporation technique to rescue the migration phenotype characterizing the *Ngn2*$^{-/-}$ cortical progenitors by expressing a dominant-negative form of RhoA (RhoA^{N19}, Olson et al., 1995). Expression of RhoA^{N19} in E14.5 cortical progenitors of *Ngn2*$^{-/-}$ embryos is sufficient to partially rescue the migration defect and induces a significant proportion of neurons to leave the VZ/SVZ and migrate into the IZ (Figures 7A–7D). However, this rescue was only partial, as most migrating neurons stopped sharply at the boundary between the IZ and the CP after 4 DIV (Figures 7B and 7D).

Because of the pronounced proneural defect characterizing *Ngn2*$^{-/-}$ cortical progenitors (Nieto et al., 2001), we wanted to determine whether we could rescue more specifically the migration phenotype due to the expression of Ngn2^{Y241F} (which does present any proneural effect) in cortical progenitors by inhibiting RhoA activity. As shown in Figure S7, coelectroporation of two constructs expressing RhoA^{N19}-IRES-EGFP and Ngn2^{Y241F}-IRES-DsRed2 leads to the high rate of coexpression of both constructs (more than 90%). Importantly, expression of RhoA^{N19} is sufficient to rescue the

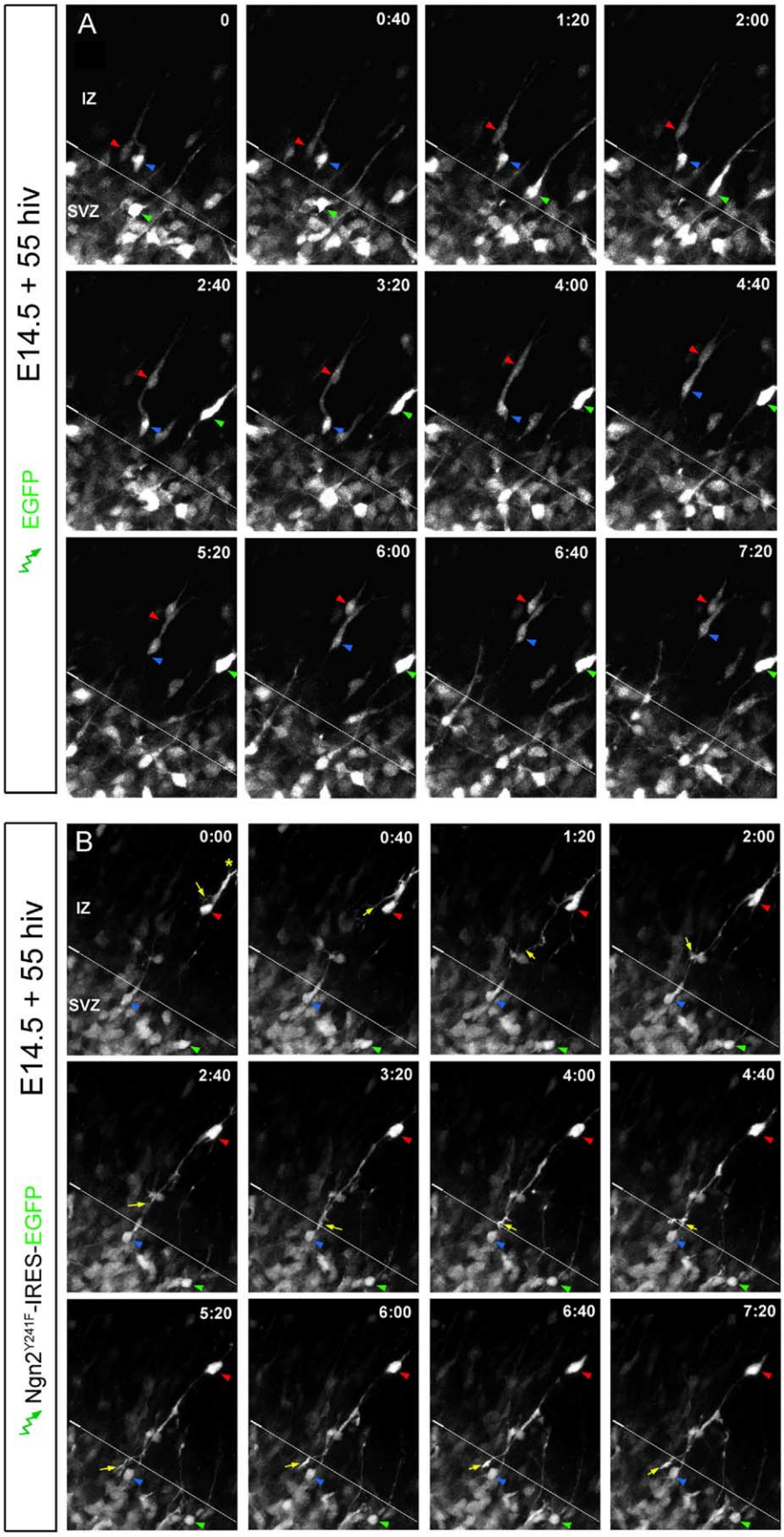
A
0
0:40
1:20
2:00
IZ
SVZ
2:40
3:20
4:00
4:40
5:20
6:00
6:40
7:20
EGFP
E14.5 + 55 hiv
B
0:00
0:40
1:20
2:00
IZ
SVZ
2:40
3:20
4:00
4:40
5:20
6:00
6:40
7:20
Ngn2Y241F-IRES-EGFP
E14.5 + 55 hiv

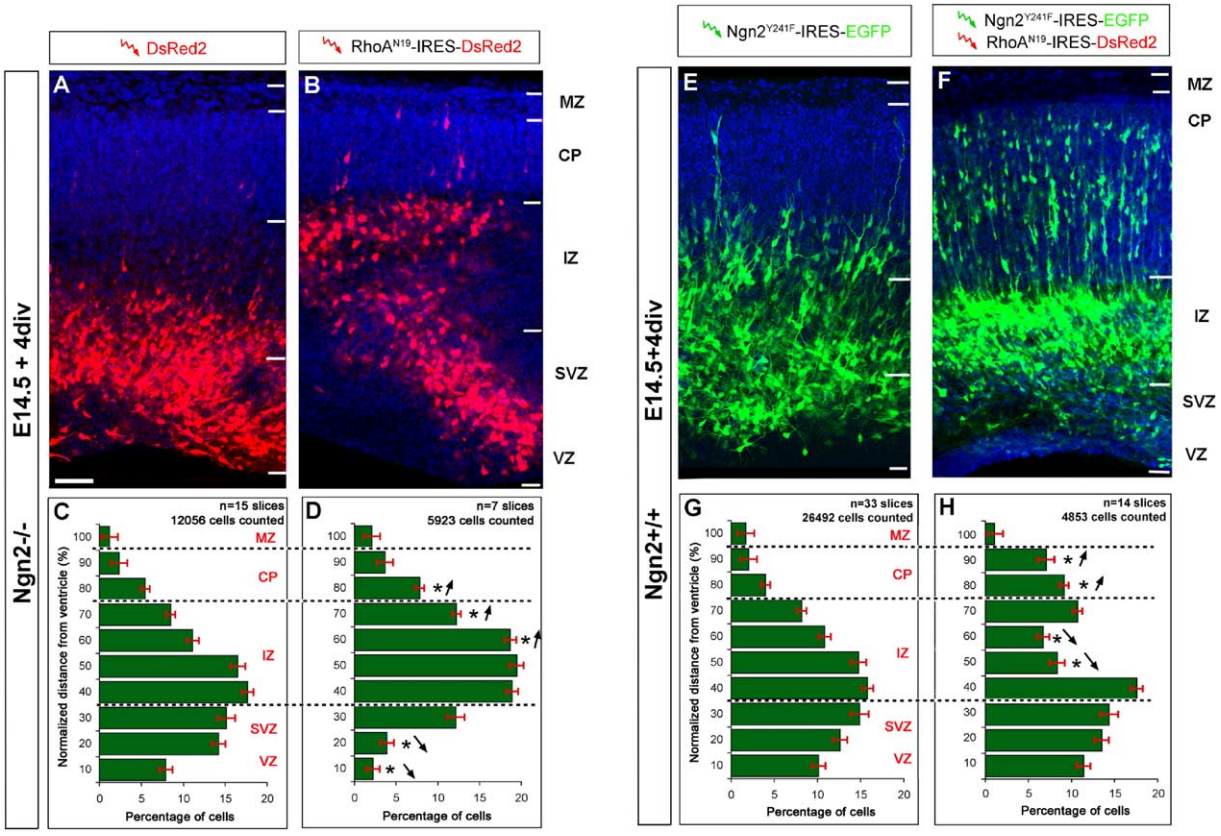

Figure 7. Inhibition of RhoA Activity Rescues the Migration Defect Due to *Ngn2* Loss of Function

(A–D) Ex vivo electroporation of dominant-negative RhoA (RhoA^{N19}-IRES-DsRed2; [B and D]) in E14.5 *Ngn2*$^{-/-}$ cortical progenitors increases the number of cells initiating migration into the IZ compared to control DsRed2 electroporation in *Ngn2*$^{-/-}$ progenitors (A and C). Note that this is a partial rescue because the majority of cells expressing RhoA^{N19} in the *Ngn2*$^{-/-}$ slices fail to enter the CP.

(E–H) Coexpression of dominant-negative RhoA^{N19}-IRES-DsRed2 and Ngn2^{Y241F}-IRES-EGFP (F–H) almost completely rescues the migration defect caused by expression of Ngn2^{Y241F} alone (E–G).

*$p < 0.01$ χ^2 test comparing equivalent bins. Scale bar in (A), (B), (E), and (F), 50 μm.

inhibition of migration due to expression of Ngn2^{Y241F} in cortical progenitors (Figures 7F–7H) to a level comparable to control electroporation of EGFP only (see Figures 5A and 5E) or wild-type Ngn2 (see Figures 5B and 5F). These results demonstrate that tyrosine 241 in Ngn2 is required for the specification of the radial migration properties of cortical progenitors at least partially by inhibiting RhoA activity.

Neurogenin2 Is Sufficient to Specify the Unipolar Dendritic Morphology of Pyramidal Neurons

In slices expressing EGFP only (Figure 8A) or full-length *Ngn2* (Figure 8B), the vast majority of neurons accumulate at the top of the CP after completion of their radial migration, where they display a unipolar morphology with their leading process/apical dendrite directed toward the marginal zone (Figures 8E and 8F, respectively). The expression of *Ngn2*$^{NR->AQ}$ resulted in a significant disorganization of the CP (Figure 8C). Importantly, expression of both *Ngn2*$^{NR->AQ}$ and *Ngn2*^{Y241F} is sufficient to induce nonpyramidal, multipolar dendritic morphologies defined by the absence of the main apical dendrite and the outgrowth of multiple primary dendrites from the cell body (red arrows in Figures 8G and 8H; see also Figure S8).

The interpretation of the effects of Ngn2^{Y241F} on den-

Figure 6. Expression of Ngn2^{Y241F} Impairs the Polarity of Neurons Initiating during Radial Migration in the Intermediate Zone

(A) Time-lapse confocal microscopy images showing the dynamics of radial migration for neurons transitioning from the SVZ to the IZ (time stamp in hours:minutes; see also Movie S1). Colored arrows (red, green, and blue) point to individual control cells electroporated with EGFP, which display the characteristic unipolar morphology of migrating neurons with a single leading process directed toward the pial surface (top of the pictures).

(B) In contrast, neurons expressing Ngn2^{Y241F} display a striking polarity defect where some cells (red arrow) lose their pre-existing leading process (pointed by asterisk in [B]) and extend a process toward the ventricle instead (yellow arrow). In addition, all three cells pointed to by arrows fail to translocate their nucleus toward the leading process and as a result fail to move during the entire duration of the movie (see also Movie S2).

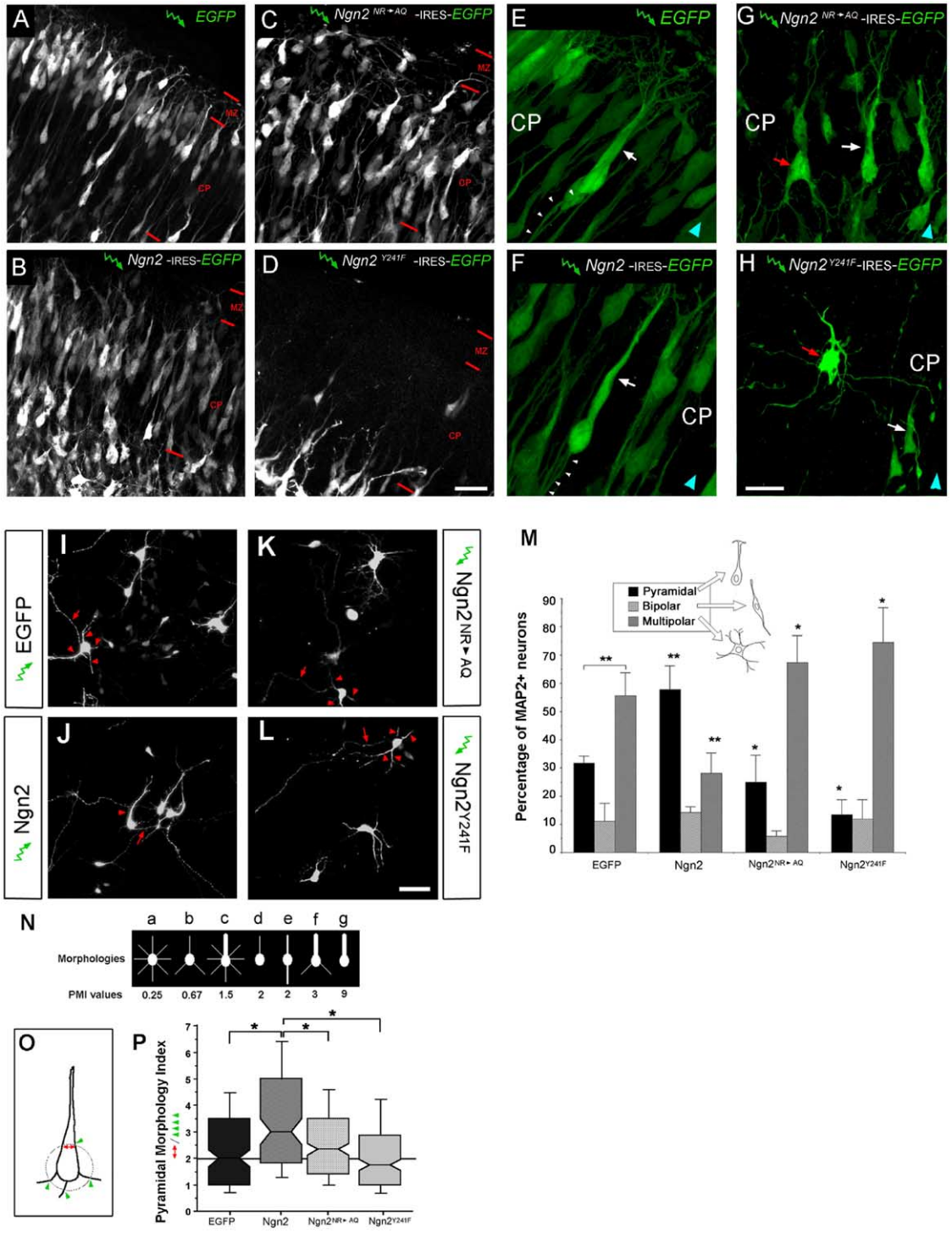

Figure 8. *Ngn2* Expression Is Sufficient to Specify a Pyramidal Dendritic Morphology

(A–D) Confocal micrographs illustrating cell organization of the CP of slices electroporated with EGFP (control; [A]), wild-type Ngn2 (B), $Ngn2^{NR->AQ}$ (C), or $Ngn2^{Y241F}$ (D).

(E–H) Precursors expressing $Ngn2^{NR->AQ}$ (G) or $Ngn2^{Y241F}$ (H) but not EGFP (E) or full-length Ngn2 (F) give rise to neurons displaying nonpyramidal, multipolar dendritic morphologies in the CP (red arrows point to nonpyramidal neurons; white arrow to pyramidal neurons). Small arrowheads point to the axon.

(I–L) E14.5 cortical progenitors electroporated with a control plasmid (EGFP) and maintained for 5 DIV in dissociated culture fail to establish a pyramidal morphology and instead display nonpyramidal morphologies with multiple, relatively thin dendritic processes (arrowheads; identified using MAP2, data not shown) and a unique, long and thin axonal process (arrow; MAP2 negative but neurofilament 165 kDa positive; data not shown). Expression of full-length Ngn2 (J) (but not $Ngn2^{NR->AQ}$ [K] or $Ngn2^{Y241F}$ [L]) is sufficient to restore the unipolar pyramidal

dritic morphology is complicated by the fact that the unipolar dendritic morphology of pyramidal neurons in the CP may depend on the ability of these neurons to respond to putative extracellular cues during migration. In order to test more directly whether *Ngn2* plays a role in the specification of the pyramidal dendritic morphology, we took advantage of the fact that previous studies have shown that in low- to medium-density dissociated cultures, cortical progenitors give rise to neurons displaying nonpyramidal/multipolar dendritic morphologies (Hayashi et al., 2002; Threadgill et al., 1997) and therefore fail to display the unipolar morphology characterizing early pyramidal neurons in vivo (Peters and Kara, 1985a; Peters et al., 1985). Interestingly, *Ngn2* transcription is significantly downregulated in dissociated cortical cultures (data not shown), raising the possibility that maintenance of proper level of *Ngn2* expression in cortical progenitors requires cell-cell contacts. We confirmed that the majority of cortical progenitors in dissociated cultures give rise to neurons displaying multipolar dendritic morphologies characterized by multiple dendrites emerging from the cell body (arrowheads in Figure 8I). Quantification using observer-based categorization (Figure 8M) revealed that only 30% of the neurons in control cultures displayed a unipolar morphology characteristic of pyramidal neurons in vivo (i.e., one large apical dendrite emerging from the cell body), approximately 10% displayed a bipolar morphology (i.e., two equally wide dendrites emerging from the cell body), and approximately 60% displayed multipolar, nonpyramidal morphologies (i.e., more than two dendrites emerging from the cell body). Strikingly, constitutive expression of *Ngn2* by electroporation in cortical progenitors is sufficient to restore the pyramidal morphology of neurons in culture, in the absence of cell-cell contacts (Figures 8J and 8M). Importantly, neither $Ngn2^{NR->AQ}$ (Figure 8K) nor $Ngn2^{Y241F}$ (Figure 8L) exerted the same activity as wild-type Ngn2, and both constructs failed to promote a unipolar morphology in cortical neurons (Figure 8M), suggesting that both the DNA binding properties and tyrosine 241 are necessary in order for Ngn2 to specify the polarized dendritic outgrowth characterizing pyramidal neurons.

The categorization of the dendritic morphologies of neurons is subjective and therefore heavily observer dependent. In order to circumvent this problem, we developed a quantitative, unbiased index called the Pyramidal Morphology Index (PMI), defined as the ratio between the width of the largest process and the total number of processes emerging from the cell body (Figure 8O). As shown in Figure 8N on model cells, the PMI value obtained for a population of cells ranging from purely multipolar (cell a) to purely unipolar (cell g) increases with the polarity of dendritic outgrowth. The measure of the width and number of processes was automated using a series of image analysis tools (see Supplemental Experimental Procedures). As shown in Figure 8P, the PMI analysis confirms the shift between multipolar morphologies observed in control (EGFP only) cultures and unipolar morphologies observed in neurons expressing full-length Ngn2 ($p = 0.0014$; ANOVA test). Importantly, expression of both $Ngn2^{NR->AQ}$ and $Ngn2^{Y241F}$ failed to increase the PMI values observed when overexpressing full-length Ngn2 (Figure 8P), confirming that Ngn2 function in the specification of pyramidal dendritic morphology requires the integrity of the DNA binding properties and the phosphorylation of tyrosine 241.

In order to correlate the morphological changes observed in dissociated cultures to those observed in slices, we measured the PMI in slices where progenitors were electroporated with EGFP only (expressing endogenous Ngn2) or $Ngn2^{Y241F}$ (Figure S8). This quantitative analysis confirms our qualitative observation reported above (see Figure 8H), i.e., the striking switch from pyramidal/unipolar (control in Figures S8A and S8C) into nonpyramidal/multipolar dendritic morphology of the few neurons transfected with $Ngn2^{Y241F}$ that reached the CP (Figure S8B and S8C).

Ngn1 Promotes Radial Migration but Does Not Promote Unipolar Dendritic Morphology to the Same Extent as Ngn2

As mentioned previously, tyrosine 241 and its surrounding proline-rich motif (YWQPPPP) are not present in Ngn1 or Ngn3. We wanted to determine whether Ngn2 function in the specification of the migration properties and the dendritic morphology of pyramidal neurons is shared by other Neurogenins. To test this we electroporated both mouse Ngn1-IRES-EGFP or Ngn2-IRES-DsRed2 at E14.5 and assessed the migration properties of cortical progenitors in organotypic slice culture. Our quantitative analysis demonstrates that Ngn1 (Figures S9A and S9C) promotes the radial migration of cortical progenitors to the same extent as Ngn2 (Figures S9B and S9D) despite minor differences in the final distribution of postmitotic neurons in the CP and MZ.

However, we found that Ngn1 does not specify py-

dendritic morphology characterized by a unique large apical process tapering away from the cell body (arrowhead in [J]) and a unique axon (arrow in [J]).

(M) Qualitative categorization of dendritic morphologies of cortical postmitotic neurons emerging from E14.5 progenitors electroporated by the constructs indicated in panels (I)–(L). *$p < 0.05$ and **$p < 0.01$; χ^2 analysis. A minimum of 200 randomly sampled neurons from four independent experiments were examined for each treatment.

(N and O) Definition of the Pyramidal Morphology Index (PMI) as a tool allowing unbiased categorization of dendritic morphology. The PMI is defined as the ratio between the width of the largest process and the total number of processes (as depicted in [O]) crossing a sampling circle of fixed diameter (25 μm).

(P) Box plots of PMI values computed for a minimum of 150 neurons per experimental set (from four independent experiments). The expression of *Ngn2* (but not $Ngn2^{NR->AQ}$ or $Ngn2^{Y241F}$) increases significantly the PMI values of neurons derived from control EGFP-expressing progenitors. *$p < 0.01$ ANOVA one-way test. Box plots indicate the median (bottleneck), the 25th, and 75th percentiles (main box) as well as the 90th and 10th percentiles (top and bottom bars, respectively).

Scale bars, 40 μm (A–D), 20 μm (E–H),and 30 μm (I–L).

ramidal dendritic morphology in dissociated E14.5 cortical cultures to the same extent as Ngn2 (Figures S9E–S9F). In fact, the PMI values obtained for progenitors expressing Ngn1 were not significantly different from control EGFP-electroporated cortical progenitors (Figure S9F), suggesting that Ngn2 is unique with regard to its ability to promote pyramidal dendritic morphology.

Discussion

Coordinated Specification of the Radial Migration Properties and Dendritic Morphology of Pyramidal Neurons

Recent time-lapse confocal analysis of the early initiation of radial migration of cortical progenitors revealed that upon cell-cycle exit immature neurons display a striking transition from a multipolar to a unipolar morphology at the level of the SVZ (Noctor et al., 2004; Tabata and Nakajima, 2003). These results strongly suggested that molecular mechanisms operating during the initiation of radial migration specify the polarity of the leading process extension and ultimately determine the unipolar dendritic morphology of pyramidal neurons in the cortex (Kriegstein and Noctor, 2004). Our results show that the coordinated initiation of radial migration and the acquisition of a unipolar leading process/apical dendrite outgrowth is dynamically controlled by posttranslational modification of Ngn2.

We found that the expression of Ngn2^{Y241F} uncouples the neuronal-subtype specification functions of *Ngn2* from its generic proneural function. Interestingly, a recent study in chick spinal cord has also shown that the proneural and the subtype specification functions of bHLH transcription factors such as Mash1 and Math1 are actually dependent on residues located outside the basic DNA binding region, in the second Helix region (Nakada et al., 2004). These results strongly suggest that (1) bHLH transcription factors such as Ngn2 are coordinating the acquisition of pan-neuronal properties through the control of the transcription of genes allowing cell cycle exit and initiation of generic pan-neuronal differentiation program (expression of MAP2, βIII-tubulin, etc.), but (2) at the same time these bHLH TFs regulate the transcription of region-specific genes specifying neuronal subtype identity, including their neurotransmitter, their molecular identity (Schuurmans et al., 2004), but also their migration properties and the dendritic morphology (present study). One of the main findings of the present study is that these two distinct functions involve different molecular modules within Ngn2.

Candidate Genes Underlying the Function of *Neurogenin2* in the Specification of Pyramidal Dendritic Morphology

What are the signaling pathways underlying the ability of *Ngn2* to promote radial migration and a pyramidal dendritic morphology? Our results provide insights into the molecular control of neuronal migration and dendritic polarity in the cortex because in our rescue experiments (Ngn2 knockout and Ngn2^{Y241F} electroporation) expression of dominant-negative RhoA is sufficient to recruit the migrating neurons into the IZ, but a lot of migrating neurons are stalled beneath the CP and seem to be unable to enter their final environment by bypassing their predecessors. This suggests a two-step model of radial migration, with a first step in which early postmitotic neurons exit the VZ/SVZ neuroepithelium and migrate into the IZ, which requires phosphorylation of Ngn2^{Y241}, leading to transient inhibition of RhoA activity through transcription of RhoGAPs and also expression of Doublecortin and other regulators of neuronal migration (Mattar et al., 2004; Bai et al., 2003); and a second step controlled by Rac1/Cdc42 activity (Kawauchi et al., 2003) in which neurons migrate through from the IZ into the CP (reviewed in Gupta et al., 2002).

Potential Signaling Pathways Involved in the DNA Binding Independent Function of Ngn2

Several studies have already illustrated the importance of protein-protein interactions and posttranslational modifications in mediating some of the biological functions of bHLH transcription factors (Lee and Pfaff, 2003; Moore et al., 2002; Olson et al., 1998; Sun et al., 2001; Talikka et al., 2002; Vojtek et al., 2003; reviewed in Puri and Sartorelli, 2000). Our results show that the DNA binding-independent function of Ngn2 in the specification of the neuronal migration properties and dendritic morphology of cortical neurons is mediated by phosphorylation of tyrosine 241. This tyrosine residue is part of a larger Ngn2-specific proline-rich domain (YWQ PPPP) motif that constitutes a predicted SH2 binding site for non-receptor tyrosine kinase (R.H. and F.P., unpublished data). Future experiments will be aimed at determining which non-receptor tyrosine kinase phosphorylates Ngn2^{Y241} and how this phosphorylation regulates Ngn2 function.

We hypothesize that the subtype specification activity mediated by phosphorylation of Ngn2^{Y241} regulates protein-protein interaction, for example, by converting a transcriptional repressor into an activator, thereby inducing the transcription of downstream target genes that regulate neuronal migration and dendritic polarity such as specific Rho-GAPs (see Figure 9). This model would explain why Ngn2^{Y241F} is acting as a dominant negative over Ngn2. Current experiments are aimed at identifying phosphorylation-dependent interactors of Ngn2^{Y241} that might mediate the transcription of specific target genes controlling radial migration and the polarity of dendritic outgrowth.

Is the Phosphorylation of Ngn2^{Y241} a Mammalian-Specific Feature?

Ngn2^{Y241} is conserved in mammals (human, rat, and mouse) but not in nonmammalian vertebrates such as birds (chick). Interestingly, neurons in the avian dorsal telencephalon accumulate according to a loose "outside-first, inside-last" sequence (Tsai et al., 1981), a pattern opposite to the inside-first, outside-last pattern characterizing all mammals (Sidman and Rakic, 1973), leading to a loosely laminated structure that lacks the six layers characterizing the mammalian neocortex. Furthermore, the avian dorsal telencephalon contains few neurons with a pyramidal morphology (Molla et al., 1986), contrasting with the mammalian neocortex where approximately 70%–80% of all cortical neurons are pyramidal (Peters and Kara, 1985a; Peters et al., 1985). The ability of migrating pyramidal neurons to de-

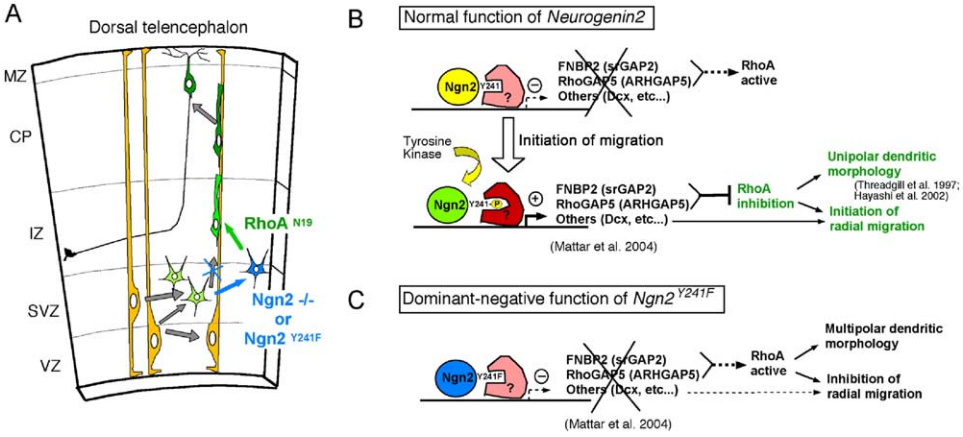

Figure 9. Proposed Model for Ngn2 Function in the Specification of the Migration Properties and the Dendritic Morphology of Pyramidal Neurons

(A) Radial glial cells (yellow) are proliferating and producing neurons through both asymmetrical division in the VZ and symmetrical neurogenic divisions in the SVZ (Kriegstein and Noctor, 2004; Malatesta et al., 2000; Miyata et al., 2004; Noctor et al., 2001, 2002, 2004). Progenitors expressing Ngn2^{Y241F} generate postmitotic neurons that fail to migrate past the IZ and present unpolarized, multipolar dendritic morphologies. These defects are significantly (but not completely, see Discussion) rescued by inhibiting RhoA activity.

(B) Potential mechanisms underlying the function of *Ngn2* in the specification of the radial migration properties and the dendritic morphology of pyramidal neurons. We hypothesize that during the initiating radial migration (B), Ngn2 is phosphorylated on tyrosine 241, which converts one of its putative interactors from a transcriptional repressor into a transcriptional activator regulating the transcription of genes that could regulate neuronal migration and dendritic polarity such as RhoGAP proteins (FNBP2 or RhoGAP5) or Doublecortin (see Mattar et al., 2004).

(C) We hypothesize that the dominant-negative effect of the Ngn2^{Y241F} mutation is due to its inability to convert the putative Ngn2-associated repressor into an activator.

velop a unipolar morphology in the IZ and bypass its predecessors by perforating the cell-dense CP (leading to an inside-out accumulation pattern) is therefore a mammalian-specific feature (Bar et al., 2000; Gupta et al., 2002). It is tempting to speculate that Ngn2^{Y241} and its surrounding motif (YWQPPPP) represent a mammalian-specific protein-protein interaction module that might have enabled the coordinated appearance of a pyramidal unipolar morphology and the inside-out laminar accumulation of neurons during brain evolution.

Finally, this motif is specific to *Ngn2*, as it is not found in the closely related *Ngn1* or *Ngn3* (Figure 4B). Interestingly, we found that *Ngn1* promotes radial migration just as efficiently as *Ngn2* but does not promote pyramidal dendritic morphology of E14.5 cortical progenitors (Figure S9). Future experiments will determine the molecular basis underlying the differences of biological activity between members of the *Neurogenin* subfamily of bHLH transcription factors in the specification of cortical neurons phenotype.

Experimental Procedures

Animals

Mice were used according to a protocol approved by the Institutional Animal Care and Use Committee at the University of North Carolina-Chapel Hill and in accordance with NIH guidelines. Time-pregnant females were maintained in a 12 hr light/dark cycle and obtained by overnight breeding with males of the same strain. Noon following breeding is considered as E0.5.

Immunofluorescence, Biochemistry, and Time-Lapse Confocal Microscopy

See Supplemental Experimental Procedures.

Constructs

All Ngn2 cDNAs were subcloned into a pCIG2 vector that we modified from the pCIG vector (kind gift of Andy McMahon; Harvard University), which contains a (cDNA)-IRES-EGFP or a (cDNA)-IRES-DsRed2 expression cassette expressed under the control of a CMV-enhancer and a chicken β-actin promoter (Megason and McMahon, 2002). The Cre recombinase coding sequence fused to SV40 nuclear localization sequence was obtained from pSK-Cre1 (a generous gift from Malcolm Logan) and inserted into pCIG2.

Ex Vivo Electroporation and Organotypic Slice Culture

Briefly, electroporation of dorsal telencephalic progenitors was performed by injecting pCIG2 plasmid DNA (1 μg/μl endotoxin-free plasmid DNA; MEGA-Prep kit from Clontech) plus 0.5% Fast Green (Sigma; 1:20 ratio) using a Picospritzer III (General Valve) microinjector into the lateral ventricles of isolated E14.5 embryonic mouse heads that were decapitated and placed in complete HBSS (see Figure S1 and Polleux and Ghosh, 2002). Electroporations were performed on the whole head (skin and skull intact) with gold-coated electrodes (GenePads 5 × 7 mm BTX; Figure S1) using an ECM 830 electroporator (BTX) and the following parameters: four 100 ms long pulses separated by 100 ms long intervals at 55 V. Immediately after electroporation, the brain was extracted and vibratome sectioned at 250 microns (LEICA VT1000S) with special care toward the integrity of the pial surface. The resulting slices were maintained in organotypic slice cultures, fixed, and stained for immunofluorescence as previously described (Polleux and Ghosh, 2002).

Dissociated Cortical Cultures

Dissociated E14.5 cortical cultures were performed using a papain-based enzymatic dissociation method as previously described (Polleux and Ghosh, 2002; Polleux et al., 2000). Dissociated and electroporated cortical progenitors were cultured on glass-bottom dishes coated with Laminin and Poly-L-Lysine for 5 days in serum-free culture medium (NeuroBasal plus B27 plus N2 supplements).

Confocal Microscopy

Fluorescent immunostaining was observed using a LEICA TCS-SL laser scanning confocal microscope equipped with an Argon laser (488 nm), green Helium-Neon laser (546nm), and red Helium-Neon laser line (633nm) for observation of Alexa-488, Alexa-546, and Alexa-647 conjugated secondary antibodies (Molecular Probes)

and Draq5 nucleic acid staining (Alexis). See Supplemental Experimental Procedures for details.

Supplemental Data

The Supplemental Data for this article can be found online at http://www.neuron.org/cgi/content/full/48/1/45/DC1/.

Acknowledgments

We are grateful to K. Burridge, A. McMahon, M.J. Tsai, and A. Ghosh for providing constructs and to Dr. Nakafuku for providing the polyclonal anti-Ngn2 antibody. We would like to thank members of the K. Burridge, L. Graves, and M. Schaller's laboratories for helpful advices. The Nestin (Rat-401) monoclonal antibody developed by Dr. S. Hockfield was obtained through the Developmental Studies Hybridoma Bank (NICHD -University of Iowa, Dept. of Biol. Sciences). This project was partially funded by the NIH-National Institute of Neurological Disorders and Stroke (NS047701-01) (F.P.), by the Confocal and Multiphoton Imaging Facility of the NINDS Institutional Center Core Grant to Support Neuroscience Research (P30 NS45892-01), the Pew Charitable Trust (F.P.), and the March of Dimes Foundation for Birth Defects (F.P.). P.M. is a recipient of a CIHR Doctoral award, L.N. is supported by a EMBO long-term fellowship, J.I.-T.H. is supported by a Postdoctoral training fellowship from Australian NHMRC. F.G.'s lab contribution was supported by MRC core funding and an European Commission RTD Program grant.

Received: November 6, 2004
Revised: May 4, 2005
Accepted: August 19, 2005
Published: October 5, 2005

References

Arthur, W.T., and Burridge, K. (2001). RhoA inactivation by p190RhoGAP regulates cell spreading and migration by promoting membrane protrusion and polarity. Mol. Biol. Cell *12*, 2711–2720.

Bai, J., Ramos, R.L., Ackman, J.B., Thomas, A.M., Lee, R.V., and LoTurco, J.J. (2003). RNAi reveals doublecortin is required for radial migration in rat neocortex. Nat. Neurosci. *6*, 1277–1283.

Bar, I., Lambert de Rouvroit, C., and Goffinet, A.M. (2000). The evolution of cortical development. An hypothesis based on the role of the Reelin signaling pathway. Trends Neurosci. *23*, 633–638.

Berry, M., and Rogers, A.W. (1965). The migration of neuroblasts in the developing cerebral cortex. J. Anat. *99*, 691–709.

Bertrand, N., Castro, D.S., and Guillemot, F. (2002). Proneural genes and the specification of neural cell types. Nat. Rev. Neurosci. *3*, 517–530.

Blom, N., Gammeltoft, S., and Brunak, S. (1999). Sequence and structure-based prediction of eukaryotic protein phosphorylation sites. J. Mol. Biol. *294*, 1351–1362.

Coyle, I.P., Koh, Y.H., Lee, W.C., Slind, J., Fergestad, T., Littleton, J.T., and Ganetzky, B. (2004). Nervous wreck, an SH3 adaptor protein that interacts with Wsp, regulates synaptic growth in Drosophila. Neuron *41*, 521–534.

des Portes, V., Pinard, J.M., Billuart, P., Vinet, M.C., Koulakoff, A., Carrie, A., Gelot, A., Dupuis, E., Motte, J., Berwald-Netter, Y., et al. (1998). A novel CNS gene required for neuronal migration and involved in X-linked subcortical laminar heterotopia and lissencephaly syndrome. Cell *92*, 51–61.

Fode, C., Gradwohl, G., Morin, X., Dierich, A., LeMeur, M., Goridis, C., and Guillemot, F. (1998). The bHLH protein NEUROGENIN 2 is a determination factor for epibranchial placode-derived sensory neurons. Neuron *20*, 483–494.

Fode, C., Ma, Q., Casarosa, S., Ang, S.L., Anderson, D.J., and Guillemot, F. (2000). A role for neural determination genes in specifying the dorsoventral identity of telencephalic neurons. Genes Dev. *14*, 67–80.

Gleeson, J.G., Allen, K.M., Fox, J.W., Lamperti, E.D., Berkovic, S., Scheffer, I., Cooper, E.C., Dobyns, W.B., Minnerath, S.R., Ross, M.E., and Walsh, C.A. (1998). Doublecortin, a brain-specific gene mutated in human X-linked lissencephaly and double cortex syndrome, encodes a putative signaling protein. Cell *92*, 63–72.

Gupta, A., Tsai, L.H., and Wynshaw-Boris, A. (2002). Life is a journey: a genetic look at neocortical development. Nat. Rev. Genet. *3*, 342–355.

Hasegawa, H., Ashigaki, S., Takamatsu, M., Suzuki-Migishima, R., Ohbayashi, N., Itoh, N., Takada, S., and Tanabe, Y. (2004). Laminar patterning in the developing neocortex by temporally coordinated fibroblast growth factor signaling. J. Neurosci. *24*, 8711–8719.

Hassan, B.A., Bermingham, N.A., He, Y., Sun, Y., Jan, Y.N., Zoghbi, H.Y., and Bellen, H.J. (2000). atonal regulates neurite arborization but does not act as a proneural gene in the Drosophila brain. Neuron *25*, 549–561.

Hatanaka, Y., and Murakami, F. (2002). In vitro analysis of the origin, migratory behavior, and maturation of cortical pyramidal cells. J. Comp. Neurol. *454*, 1–14.

Hausser, M., Spruston, N., and Stuart, G.J. (2000). Diversity and dynamics of dendritic signaling. Science *290*, 739–744.

Hayashi, K., Ohshima, T., and Mikoshiba, K. (2002). Pak1 is involved in dendrite initiation as a downstream effector of Rac1 in cortical neurons. Mol. Cell. Neurosci. *20*, 579–594.

Huang, H.P., Liu, M., El-Hodiri, H.M., Chu, K., Jamrich, M., and Tsai, M.J. (2000a). Regulation of the pancreatic islet-specific gene BETA2 (neuroD) by neurogenin 3. Mol. Cell. Biol. *20*, 3292–3307.

Huang, M.L., Hsu, C.H., and Chien, C.T. (2000b). The proneural gene amos promotes multiple dendritic neuron formation in the Drosophila peripheral nervous system. Neuron *25*, 57–67.

Jan, Y.N., and Jan, L.Y. (2003). The control of dendrite development. Neuron *40*, 229–242.

Jarman, A.P., Grau, Y., Jan, L.Y., and Jan, Y.N. (1993). atonal is a proneural gene that directs chordotonal organ formation in the Drosophila peripheral nervous system. Cell *73*, 1307–1321.

Katoh, M. (2004). Identification and characterization of human FCHSD1 and FCHSD2 genes in silico. Int. J. Mol. Med. *13*, 749–754.

Kawauchi, T., Chihama, K., Nabeshima, Y., and Hoshino, M. (2003). The in vivo roles of STEF/Tiam1, Rac1 and JNK in cortical neuronal migration. EMBO J. *22*, 4190–4201.

Kriegstein, A.R., and Noctor, S.C. (2004). Patterns of neuronal migration in the embryonic cortex. Trends Neurosci. *27*, 392–399.

Lee, S.K., and Pfaff, S.L. (2003). Synchronization of neurogenesis and motor neuron specification by direct coupling of bHLH and homeodomain transcription factors. Neuron *38*, 731–745.

Ma, Q., Fode, C., Guillemot, F., and Anderson, D.J. (1999). Neurogenin1 and neurogenin2 control two distinct waves of neurogenesis in developing dorsal root ganglia. Genes Dev. *13*, 1717–1728.

Malatesta, P., Hartfuss, E., and Gotz, M. (2000). Isolation of radial glial cells by fluorescent-activated cell sorting reveals a neuronal lineage. Development *127*, 5253–5263.

Marin, O., and Rubenstein, J.L. (2003). Cell migration in the forebrain. Annu. Rev. Neurosci. *26*, 441–483.

Mattar, P., Britz, O., Johannes, C., Nieto, M., Ma, L., Rebeyka, A., Klenin, N., Polleux, F., Guillemot, F., and Schuurmans, C. (2004). A screen for downstream effectors of Neurogenin2 in the embryonic neocortex. Dev. Biol. *273*, 373–389.

Megason, S.G., and McMahon, A.P. (2002). A mitogen gradient of dorsal midline Wnts organizes growth in the CNS. Development *129*, 2087–2098.

Miller, M. (1981). Maturation of rat visual cortex. I. A quantitative study of Golgi-impregnated pyramidal neurons. J. Neurocytol. *10*, 859–878.

Miller, M.W. (1986). Maturation of rat visual cortex. III. Postnatal morphogenesis and synaptogenesis of local circuit neurons. Brain Res. *390*, 271–285.

Miyata, T., Kawaguchi, A., Saito, K., Kawano, M., Muto, T., and Ogawa, M. (2004). Asymmetric production of surface-dividing and

non-surface-dividing cortical progenitor cells. Development *131*, 3133–3145.

Mizuguchi, R., Sugimori, M., Takebayashi, H., Kosako, H., Nagao, M., Yoshida, S., Nabeshima, Y., Shimamura, K., and Nakafuku, M. (2001). Combinatorial roles of olig2 and neurogenin2 in the coordinated induction of pan-neuronal and subtype-specific properties of motoneurons. Neuron *31*, 757–771.

Molla, R., Garcia-Verdugo, J.M., Lopez-Garcia, C., and Martin-Perez, V. (1986). Neuronal development of the chick cerebral cortex. A Golgi study. J. Hirnforsch. *27*, 625–637.

Moore, K.B., Schneider, M.L., and Vetter, M.L. (2002). Posttranslational mechanisms control the timing of bHLH function and regulate retinal cell fate. Neuron *34*, 183–195.

Murciano, A., Zamora, J., Lopez-Sanchez, J., and Frade, J.M. (2002). Interkinetic nuclear movement may provide spatial clues to the regulation of neurogenesis. Mol. Cell. Neurosci. *21*, 285–300.

Nakada, Y., Hunsaker, T.L., Henke, R.M., and Johnson, J.E. (2004). Distinct domains within Mash1 and Math1 are required for function in neuronal differentiation versus neuronal cell-type specification. Development *131*, 1319–1330.

Nieto, M., Schuurmans, C., Britz, O., and Guillemot, F. (2001). Neural bHLH genes control the neuronal versus glial fate decision in cortical progenitors. Neuron *29*, 401–413.

Noctor, S.C., Flint, A.C., Weissman, T.A., Dammerman, R.S., and Kriegstein, A.R. (2001). Neurons derived from radial glial cells establish radial units in neocortex. Nature *409*, 714–720.

Noctor, S.C., Flint, A.C., Weissman, T.A., Wong, W.S., Clinton, B.K., and Kriegstein, A.R. (2002). Dividing precursor cells of the embryonic cortical ventricular zone have morphological and molecular characteristics of radial glia. J. Neurosci. *22*, 3161–3173.

Noctor, S.C., Martinez-Cerdeno, V., Ivic, L., and Kriegstein, A.R. (2004). Cortical neurons arise in symmetric and asymmetric division zones and migrate through specific phases. Nat. Neurosci. *7*, 136–144.

Olenik, C., Aktories, K., and Meyer, D.K. (1999). Differential expression of the small GTP-binding proteins RhoA, RhoB, Cdc42u and Cdc42b in developing rat neocortex. Brain Res. Mol. Brain Res. *70*, 9–17.

Olson, E.C., Schinder, A.F., Dantzker, J.L., Marcus, E.A., Spitzer, N.C., and Harris, W.A. (1998). Properties of ectopic neurons induced by Xenopus neurogenin1 misexpression. Mol. Cell. Neurosci. *12*, 281–299.

Olson, M.F., Ashworth, A., and Hall, A. (1995). An essential role for Rho, Rac, and Cdc42 GTPases in cell cycle progression through G1. Science *269*, 1270–1272.

Parras, C.M., Schuurmans, C., Scardigli, R., Kim, J., Anderson, D.J., and Guillemot, F. (2002). Divergent functions of the proneural genes Mash1 and Ngn2 in the specification of neuronal subtype identity. Genes Dev. *16*, 324–338.

Peters, A., and Kara, D.A. (1985a). The neuronal composition of area 17 of rat visual cortex. I. The pyramidal cells. J. Comp. Neurol. *234*, 218–241.

Peters, A., and Kara, D.A. (1985b). The neuronal composition of area 17 of rat visual cortex. II. The nonpyramidal cells. J. Comp. Neurol. *234*, 242–263.

Peters, A., Kara, D.A., and Harriman, K.M. (1985). The neuronal composition of area 17 of rat visual cortex. III. Numerical considerations. J. Comp. Neurol. *238*, 263–274.

Polleux, F., and Ghosh, A. (2002). The slice overlay assay: a versatile tool to study the influence of extracellular signals on neuronal development. Sci. STKE 2002, PL9.

Polleux, F., Dehay, C., and Kennedy, H. (1997). The timetable of laminar neurogenesis contributes to the specification of cortical areas in mouse isocortex. J. Comp. Neurol. *385*, 95–116.

Polleux, F., Morrow, T., and Ghosh, A. (2000). Semaphorin 3A is a chemoattractant for cortical apical dendrites. Nature *404*, 567–573.

Puri, P.L., and Sartorelli, V. (2000). Regulation of muscle regulatory factors by DNA-binding, interacting proteins, and post-transcriptional modifications. J. Cell. Physiol. *185*, 155–173.

Quan, X.J., Denayer, T., Yan, J., Jafar-Nejad, H., Philippi, A., Lichtarge, O., Vleminckx, K., and Hassan, B.A. (2004). Evolution of neural precursor selection: functional divergence of proneural proteins. Development *131*, 1679–1689.

Ridley, A.J., Schwartz, M.A., Burridge, K., Firtel, R.A., Ginsberg, M.H., Borisy, G., Parsons, J.T., and Horwitz, A.R. (2003). Cell migration: integrating signals from front to back. Science *302*, 1704–1709.

Ross, S.E., Greenberg, M.E., and Stiles, C.D. (2003). Basic helix-loop-helix factors in cortical development. Neuron *39*, 13–25.

Scardigli, R., Schuurmans, C., Gradwohl, G., and Guillemot, F. (2001). Crossregulation between Neurogenin2 and pathways specifying neuronal identity in the spinal cord. Neuron *31*, 203–217.

Schuurmans, C., and Guillemot, F. (2002). Molecular mechanisms underlying cell fate specification in the developing telencephalon. Curr. Opin. Neurobiol. *12*, 26–34.

Schuurmans, C., Armant, O., Nieto, M., Stenman, J.M., Britz, O., Klenin, N., Brown, C., Langevin, L.M., Seibt, J., Tang, H., et al. (2004). Sequential phases of cortical specification involve Neurogenin-dependent and -independent pathways. EMBO J. *23*, 2892–2902.

Scott, E.K., and Luo, L. (2001). How do dendrites take their shape? Nat. Neurosci. *4*, 359–365.

Seibt, J., Schuurmans, C., Gradwhol, G., Dehay, C., Vanderhaeghen, P., Guillemot, F., and Polleux, F. (2003). Neurogenin2 specifies the connectivity of thalamic neurons by controlling axon responsiveness to intermediate target cues. Neuron *39*, 439–452.

Sharma, A., Moore, M., Marcora, E., Lee, J.E., Qiu, Y., Samaras, S., and Stein, R. (1999). The NeuroD1/BETA2 sequences essential for insulin gene transcription colocalize with those necessary for neurogenesis and p300/CREB binding protein binding. Mol. Cell. Biol. *19*, 704–713.

Shu, T., Ayala, R., Nguyen, M.D., Xie, Z., Gleeson, J.G., and Tsai, L.H. (2004). Ndel1 operates in a common pathway with LIS1 and cytoplasmic dynein to regulate cortical neuronal positioning. Neuron *44*, 263–277.

Sidman, R.L., and Rakic, P. (1973). Neuronal migration, with special reference to developing human brain: a review. Brain Res. *62*, 1–35.

Sun, Y., Nadal-Vicens, M., Misono, S., Lin, M.Z., Zubiaga, A., Hua, X., Fan, G., and Greenberg, M.E. (2001). Neurogenin promotes neurogenesis and inhibits glial differentiation by independent mechanisms. Cell *104*, 365–376.

Tabata, H., and Nakajima, K. (2001). Efficient in utero gene transfer system to the developing mouse brain using electroporation: visualization of neuronal migration in the developing cortex. Neuroscience *103*, 865–872.

Tabata, H., and Nakajima, K. (2003). Multipolar migration: the third mode of radial neuronal migration in the developing cerebral cortex. J. Neurosci. *23*, 9996–10001.

Talikka, M., Perez, S.E., and Zimmerman, K. (2002). Distinct patterns of downstream target activation are specified by the helix-loop-helix domain of proneural basic helix-loop-helix transcription factors. Dev. Biol. *247*, 137–148.

Threadgill, R., Bobb, K., and Ghosh, A. (1997). Regulation of dendritic growth and remodeling by Rho, Rac, and Cdc42. Neuron *19*, 625–634.

Tsai, H.M., Garber, B.B., and Larramendi, L.M. (1981). ^{3}H-thymidine autoradiographic analysis of telencephalic histogenesis in the chick embryo: I. Neuronal birthdates of telencephalic compartments in situ. J. Comp. Neurol. *198*, 275–292.

Vojtek, A.B., Taylor, J., DeRuiter, S.L., Yu, J.Y., Figueroa, C., Kwok, R.P., and Turner, D.L. (2003). Akt regulates basic helix-loop-helix transcription factor-coactivator complex formation and activity during neuronal differentiation. Mol. Cell. Biol. *23*, 4417–4427.

Whitford, K.L., Dijkhuizen, P., Polleux, F., and Ghosh, A. (2002). Molecular control of cortical dendrite development. Annu. Rev. Neurosci. *25*, 127–149.

Wong, R.O., and Ghosh, A. (2002). Activity-dependent regulation of dendritic growth and patterning. Nat. Rev. Neurosci. *3*, 803–812.

Wong, K., Ren, X.R., Huang, Y.Z., Xie, Y., Liu, G., Saito, H., Tang, H., Wen, L., Brady-Kalnay, S.M., Mei, L., et al. (2001). Signal transduction in neuronal migration: roles of GTPase activating proteins and the small GTPase Cdc42 in the Slit-Robo pathway. Cell *107*, 209–221.